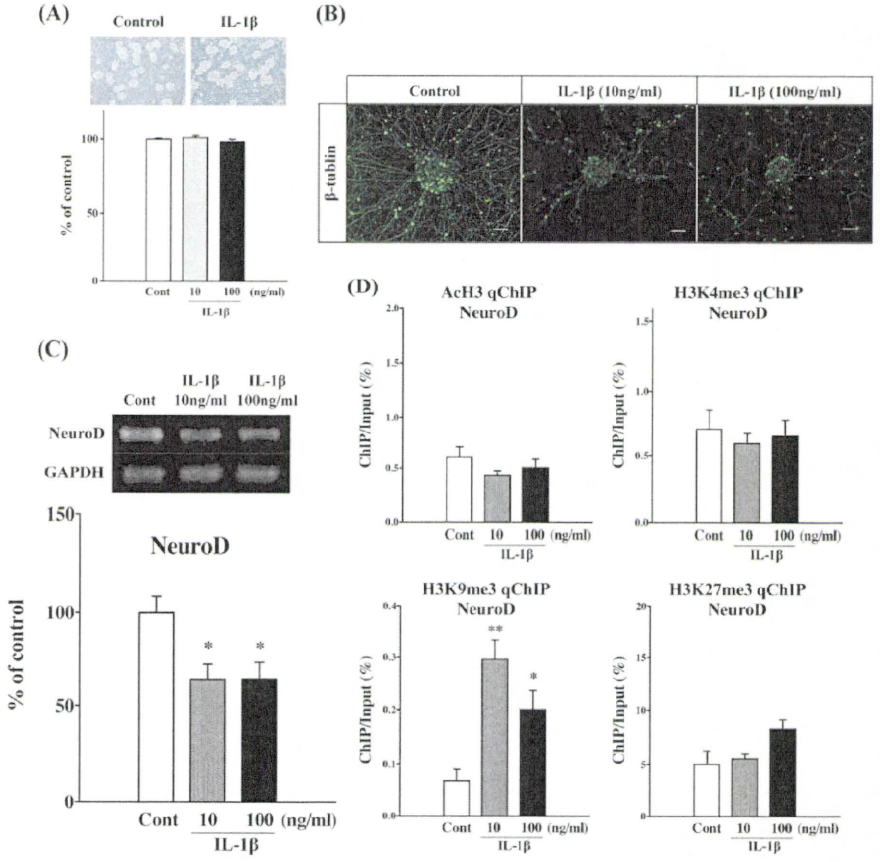

Fig. 3. **A**: Cell viability of neural stem cells after 1 day in the presence of 10 or 100 ng/ml IL-1β. Note that the IL-1β concentration has no effect on the survival of neural stem cells as indicated by Cell viability assay. **B**: Effects of IL-1β on the differentiation of neural stem cells into β-tubulin-positive neurons. The cells were incubated overnight in medium containing epidermal growth factor (EGF) that was replaced with medium alone or medium containing IL-1β (10, 100 ng/ml). Treatment with 10 or 100 ng/ml IL-1β decreased β-tubulin-positive neurons when compared with control cultures. **C**: *Upper*: Representative RT-PCR for NeuroD mRNA in neural stem cells. *Lower*: The intensity of the bands was semi-quantified using NIH Image software. The value for mRNA was normalized by that for the internal standard GAPDH mRNA. Each column represents the mean ± SEM of three samples. (*$P < 0.05$ vs. control group). **D**: qChIP analysis of AcH3, H3K4me3, H3K9me3, and H3K27me3 at NeuroD loci in neural stem cells incubated with IL-1β compared to that in control groups. The value for ChIP/Input was normalized by that for the internal standard in each control. Each column represents the mean ± SEM of 3 samples (*$P < 0.05$, **$P < 0.01$ vs. control group).

result, we detected no changes in two active histone modifications (acetylation of histone H3: AcH3, and trimethylation of lysine 4 on histone H3: H3K4) or in two repressive histone modifications (trimethylation of lysine 9 on histone H3: H3K9 and trimethylation of lysine 27 on histone H3: H3K27). Under these conditions, we found that mRNA expression of NeuroD, a neural progenitor cell marker, was significantly decreased in the hippocampus of aged mice compared with that in young mice ($P < 0.01$; Fig. 2C). In agreement with the PCR assay, we detected a significant increase in H3K9 trimethylation at the NeuroD promoter in the hippocampus of aged mice compared with that in young mice ($P < 0.05$; Fig. 2D). In contrast, we observed no changes in other histone modifications at the NeuroD gene promoter (Fig. 2D).

To further determine whether IL-1β could suppress neural stem cell proliferation and neural differentiation, we used neural stem cells prepared from whole brain of E14.5 mice. For the proliferation experiments, EGF (10 ng/ml) was used to keep the cultures proliferating. Under these conditions, treatment with IL-1β (1–100 ng/ml) failed to change the proliferation of neural stem cells as detected by a microtiter plate-based cell-survival assay (Fig. 3A). For the differentiation experiments, approximately 10 neurospheres of the same size were plated onto 10 μg/ml laminin-coated glass slides, and 400 μl of serum-free

medium with 10 ng/ml EGF was then added to each well. The neural stem cells were incubated overnight in medium with 10 ng/ml EGF and then replaced with medium alone or medium containing IL-1β (10–100 ng/ml). Treatment with IL-1β for 7 days produced a significant decrease in IR for the differentiated neural cell marker βIII-tubulin (Fig. 3B).

Under this condition, we next investigated the effects of treatment with IL-1β in neural stem cells on NeuroD mRNA expression in neural progenitor cells. Treatment with IL-1β significantly decreased the mRNA expression of NeuroD ($P < 0.05$; Fig. 3C). We next studied histone modifications at the NeuroD promoter. In agreement with the results in the aged brain, we found a significant increase in H3K9 trimethylation at the NeuroD promoter in neural stem cells that had been incubated with IL-1β compared to that in control groups ($P < 0.05$, $P < 0.01$; Fig. 3D).

Microglia constantly survey the microenvironment for noxious agents or injurious processes (Nimmerjahn et al., 2005). With aging, microglia are thought to increase in number and become activated, and may enter a phagocytic or reactive stage (Lucin and Wyss-Coray, 2009). In this study, Iba1-positive microglia were significantly increased in the DG of the hippocampus of aged mice.

Based on the activation stimuli, microglia are informed of the encountered problem and instructed to act in an appropriate manner and perform a defined task. If the disturbance is relatively minor, microglia may secrete anti-inflammatory cytokines and supportive growth factors (Lucin and Wyss-Coray, 2009). If the disturbance poses a serious threat, such as a pathogen invasion, microglia may release toxic factors to kill the pathogen and recruit help by releasing proinflammatory cytokines. If we consider the continuum of potential microglial responses, how a given insult is interpreted can mean the difference between a beneficial outcome or a detrimental outcome if the response is either too aggressive or too passive.

As well as microglia, aging caused a dramatic increase in GFAP-positive IR that is located in dendritic astrocytes, with an expanding distribution in the hippocampus of aged mice. Each individual astrocyte labeled by GFAP was branched, which indicates the activation of astrocytes in the hippocampus of aged mice. This notion is supported by a previous finding that in humans the GFAP level increases dramatically after the age of 65 years, and more specifically in the hippocampal formation (David et al., 1997). Furthermore, aging had a differential effects on astrocytic and microglial hyperactivity in gray vs. white matter areas. This mosaic of glial aging suggests that multiple mechanisms are at work during aging.

The activation of microglia or astrocytes that secrete and express numerous regulatory ligands can affect cells of immune or nonimmune tissues, such as neurons through the release of cytokines and chemokines. Cytokines and chemokines have been classified as molecules that coordinate inflammatory and immune responses, and also mediate normal, ongoing signaling between cells of nonimmune tissues (Bodles and Barger, 2004). In this study, the mRNA level of IL-1β in the hippocampus was significantly increased by aging. This result is partly supported by previous findings (Murray and Lynch, 1998).

Epigenetic alterations of DNA play key roles in determining gene structure and expression (Jaenisch and Bird, 2003; Tsankova et al., 2007). A major epigenetic modification, chromatin remodeling, modulates gene expression with high temporal and spatial resolution by permitting small groups of nucleosomes to become more or less open, which consequently enhances or inhibits access of the transcriptional machinery to specific promoter regions. The acetylation and methylation of histone proteins at specific residues play a major role in chromatin remodeling. Lysine acetylation almost always correlates with chromatin accessibility and transcriptional activity, whereas lysine methylation can have different effects depending on which residue is modified (Jenuwein and Allis, 2001). Trimethylation of H3K4 is associated with transcribed chromatin (Li et al., 2007). In contrast, trimethylation of H3K9 and H3K27 generally correlates with repression (Bernstein et al., 2005). In this study, aging did not cause any changes in the acetylation or methylation of histone proteins at any genes of IL-1β. Gene expression has been considered to be mediated through the complex machinery, which is regulated in a coordinated manner by transcription factors, protein kinases and cotranscriptional factors, which are classified as epigenetic modulators. Thus, gene transcription can be controlled by transcriptional factors singly or in combination with other transcriptional factor and protein kinases (Wang et al., 2009). With regard to such complex machinery, we hypothesize that the increased expression of IL-1β mRNA observed in the hippocampus of aged mice may be modulated by activated transcription factors with or without protein kinases, other than epigenetic modifications.

We previously reported that aging decreased the expression of the migrated neural progenitor doublecortin in association with a significant decrease in H3K4 trimethylation and a significant increase in H3K27 trimethylation in the hippocampus (Kuzumaki et al., 2010). In this study, we found that aging induced a significant increase in H3K9 trimethylation at the promoter of another neural progenitor cell marker (NeuroD) in the hippocampus. These findings suggest that aging causes the epigenetically repressive modulation of neural progenitors in the hippocampus.

We finally investigated whether IL-1β could affect neural progenitor cells through epigenetic regulation. In vitro treatment of neural stem cells prepared from whole brain of E14.5 mice with IL-1β significantly increased H3K9 trimethylation at the NeuroD promoter. These findings suggest that IL-1β, which may be produced by aging, decreases neural progenitor cells through epigenetic modulation. It has been reported that IL-1β suppresses the proliferation of hippocampal progenitor cells (Koo and Duman, 2008). It has generally been accepted that the decreased proliferation of neural stem cells is responsible for decreased neural differentiation, and increased prolifiration could correspond to the promotion of neurogenesis. In this study, treatment with 10–100 ng/ml of IL-1β produced a significant decrease in neural differentiation with no change in the proliferation of neural stem cells. This apparent discrepancy may be the result of the relatively short exposure time to IL-1β in the present cell survival assay. However, we can not deny the possibility that epigenetic modification at the NeuroD promoter by IL-1β may lead to a direct change in the neurogenesis/gliogenesis ratio or that IL-1β may promote neural differentiation from neural stem cells without affecting the survival/proliferation of neural stem cells via "unknown pathways."

In conclusion, this study demonstrated that microglia and astrocytes were activated in the DG of the hippocampus of aged mice. Furthermore, aging significantly increased mRNA levels of IL-1β without related histone modifications and increased H3K9 trimethylation at the promoter of a neural progenitor cell marker (NeuroD) in the hippocampus of aged mice. Moreover, in vitro treatment of neural stem cells prepared from whole brain of E14.5 mice with IL-1β significantly increased H3K9 trimethylation at the NeuroD promoter. These findings suggest that aging may activate microglia and astrocytes with an increased expression of IL-1β in the hippocampus. Furthermore, increased IL-1β could lead to a decrease in hippocampal neurogenesis via epigenetic modifications.

REFERENCES

Bernstein BE, Kamal M, Lindblad-Toh K, Bekiranov S, Bailey DK, Huebert DJ, McMahon S, Karlsson EK, Kulbokas EJ III, Gingeras TR, Schreiber SL, Lander ES. 2005. Genomic maps and comparative analysis of histone modifications in human and mouse. Cell 120:169–181.

Bodles AM, Barger SW. 2004. Cytokines and the aging brain–what we don't know might help us. Trends Neurosci 27:621–626.

David JP, Ghozali F, Fallet-Bianco C, Wattez A, Delaine S, Boniface B, Di Menza C, Delacourte A. 1997 Glial reaction in the hippocampal formation is highly correlated with aging in human brain. Neurosci Lett 235:53–56.

Eriksson PS, Perfilieva E, Bjork-Eriksson T, Alborn AM, Nordborg C, Peterson DA, Gage FH. 1998. Neurogenesis in the adult human hippocampus. Nat Med 4:1313–1317.

Jaenisch R, Bird A. 2003. Epigenetic regulation of gene expression: how the genome integrates intrinsic and environmental signals. Nat Genet 33 Suppl:245–254.

Jenuwein T, Allis CD. 2001. Translating the histone code. Science 293:1074–1080.

Koo JW, Duman RS. 2008. IL-1beta is an essential mediator of the antineurogenic and anhedonic effects of stress. Proc Natl Acad Sci USA 105:751–756.

Kuhn HG, Dickinson-Anson H, Gage FH. 1996. Neurogenesis in the dentate gyrus of the adult rat: age-related decrease of neuronal progenitor proliferation. J Neurosci 16:2027–2033.

Kuzumaki N, Ikegami D, Tamura R, Sasaki T, Niikura K, Narita M, Miyashita K, Imai S, Takeshima H, Ando T, Igarashi K, Kanno J, Ushijima T, Suzuki T, Narita M. 2010. Hippocampal epigenetic modification at the doublecortin gene is involved in the impairment of neurogenesis with aging. Synapse (in press).

Li B, Carey M, Workman JL. 2007. The role of chromatin during transcription. Cell 128:707–719.

Lucin KM, Wyss-Coray T. 2009. Immune activation in brain aging and neurodegeneration: Too much or too little? Neuron 64: 110–122.

Murray CA, Lynch MA. 1998. Evidence that increased hippocampal expression of the cytokine interleukin-1 beta is a common trigger for age- and stress-induced impairments in long-term potentiation. J Neurosci 18:2974–2981.

Nakajima T, Yamashita S, Maekita T, Niwa T, Nakazawa K, Ushijima T. 2009. The presence of a methylation fingerprint of Helicobacter pylori infection in human gastric mucosae. Int J Cancer 124:905–910.

Nimmerjahn A, Kirchhoff F, Helmchen F. 2005. Resting microglial cells are highly dynamic surveillants of brain parenchyma in vivo. Science 308:1314–1318.

Takeshima H, Yamashita S, Shimazu T, Niwa T, Ushijima T. 2009. The presence of RNA polymerase II, active or stalled, predicts epigenetic fate of promoter CpG islands. Genome Res 19:1974–1982.

Tsankova NM, Kumar A, Nestler EJ. 2004. Histone modifications at gene promoter regions in rat hippocampus after acute and chronic electroconvulsive seizures. J Neurosci 24:5603–5610.

Tsankova N, Renthal W, Kumar A, Nestler EJ. 2007. Epigenetic regulation in psychiatric disorders. Nat Rev Neurosci 8:355–367.

Wang K, Saito M, Bisikirska BC, Alvarez MJ, Lim WK, Rajbhandari P, Shen Q, Nemenman I, Basso K, Margolin AA, Klein U, Dalla-Favera R, Califano A. 2009. Genome-wide identification of post-translational modulators of transcription factor activity in human B cells. Nat Biotechnol 27:829–839.

SYNAPSE 64:611–616 (2010)

Hippocampal Epigenetic Modification at the Doublecortin Gene is Involved in the Impairment of Neurogenesis With Aging

NAOKO KUZUMAKI,[1] DAIGO IKEGAMI,[1] RIE TAMURA,[1] TAKUYA SASAKI,[1] KEIICHI NIIKURA,[1] MICHIKO NARITA,[1] KAZUHIKO MIYASHITA,[1] SATOSHI IMAI,[1] HIDEYUKI TAKESHIMA,[2] TAKAYUKI ANDO,[2] KATSUHIDE IGARASHI,[3] JUN KANNO,[3] TOSHIKAZU USHIJIMA,[2] TSUTOMU SUZUKI,[1]* AND MINORU NARITA[1]*

[1]*Department of Toxicology, Hoshi University School of Pharmacy and Pharmaceutical Sciences, Shinagawa-Ku, Tokyo 142-8501, Japan*

[2]*Carcinogenesis Division, National Cancer Center Research Institute, Chuo-Ku, Tokyo 104-0045, Japan*

[3]*Division of Cellular and Molecular Toxicology, Biological Safety Research Center, National Institute of Health Sciences, Setagaya-Ku, Tokyo 154-0000, Japan*

KEY WORDS senescent; mouse hippocampus; epigenome; DCX; neurogenesis

ABSTRACT Recent research has suggested that epigenetic mechanisms, which exert lasting control over gene expression without altering the genetic code, could mediate stable changes in brain function. A growing body of evidence supports the idea that epigenetic changes play a role in the etiology of aging and its associated brain dysfunction. The present study was undertaken to evaluate the age-related changes in the expression of doublecortin, which is a marker for neuronal precursors, along with epigenetic modification in the hippocampus of aged mice. In the present study, the doublecortin-positive cells were almost completely absent from the dentate gyrus of the hippocampus of 28-month-old mice. Furthermore, the expression level of doublecortin mRNA was significantly decreased in the hippocampus of aged mice. Under these conditions, a significant decrease in H3K4 trimethylation and a significant increase in H3K27 trimethylation at doublecortin promoters were observed with aging without any changes in the expression of their associated histone methylases and demethylases in the hippocampus. These findings suggest that aging produces a dramatic decrease in the expression of doublecortin along with epigenetic modifications in the hippocampus. **Synapse 64:611–616, 2010.**

INTRODUCTION

Since the average human life span has increased dramatically over the last century, there are growing concerns about malfunctions associated with aging. The dysfunction of neurotransmission in normal aging and neuropsychiatric diseases late in life may contribute to the behavioral changes commonly observed in the elderly.

Neurogenesis occurs in specific areas in the adult brain throughout life, e.g., in the subventricular zone at the telencephalic level and in the dentate gyrus of the hippocampus (Eriksson et al., 1998; Lois and Alvarez-Buylla, 1993). The dentate gyrus, the hippocampus proper, and the subiculum constitute the hippocampal formation, which is critical for certain forms of learning and memory (Bliss and Collingridge, 1993). A positive correlation has been established between neurogenesis in the dentate gyrus and an animal's performance in behavioral tasks (Kempermann et al., 1997; van Praag et al., 1999). Aging is associated with a progressive accumulation of damaged molecules and impaired energy metabolism in brain cells. Neurons and glial cells may adapt to the adversities of aging by compensating for lost or damaged cells by producing new neurons and glia, and remodeling neuronal circuits.

The influence of age on rates of neurogenesis has been studied by several groups (Kuhn et al., 1996; Lichtenwalner et al., 2001). Changes in the relative proportion of young dentate gyrus neurons may have important consequences for hippocampal function and could possibly contribute to age-dependent structural

*Correspondence to: Minoru Narita, PhD, or Tsutomu Suzuki, PhD, Department of Toxicology, Hoshi University School of Pharmacy and Pharmaceutical Sciences, Tokyo. E-mail: narita@hoshi.ac.jp/suzuki@hoshi.ac.jp

Received 14 October 2009; Accepted 17 November 2009

DOI 10.1002/syn.20768

Published online 17 March 2010 in Wiley InterScience (www.interscience.wiley.com).

and functional hippocampal deficits (Barnes, 1994; Geinisman et al., 1992).

Epigenetic changes involve transmissible alterations in gene expression caused by mechanisms other than changes in the DNA sequence. (Gravina and Vijg, 2009) Epigenetic information is destined to change during development and in the course of essential somatic functions. This makes it a more likely candidate for errors than its more stable DNA-sequence counterpart, changes in which have been well documented and increase during aging (Gravina and Vijg, 2009). Indeed, epegenomic alterations are now becoming increasingly recognized as part of aging and its associated pathologic phenotypes (Gravina and Vijg, 2009). To better understand such age-dependent epigenetic modification, in this study we focused on the decreased expression of doublecortin, which is frequently used as a marker of a migrated neuronal progenitor in the hippocampus of aged mice.

This study was conducted in accordance with the Guiding Principles for the Care and Use of Laboratory Animals, Hoshi University, as adopted by the Committee on Animal Research of Hoshi University, which is accredited by the Ministry of Education, Culture, Sports, Science and Technology of Japan. All efforts were made to minimize the number of animals used and their suffering.

Two- and from 24- to 28-month-old C57BL/6J mice were used in the present study. Animals were kept in a room with an ambient temperature of 23 ± 1°C and a 12-h light/dark cycle (lights on 8:00 AM to 8:00 PM). Food and water were available ad libitum.

Mice were deeply anesthetized with isoflurane (3%) and perfusion-fixed with 4% paraformaldehyde (pH 7.4). The brain was then removed quickly and the hippocampus was rapidly dissected and postfixed in 4% paraformaldehyde for 2 h. The hippocampus was permeated with 20% sucrose for 1 day and 30% sucrose for 2 days, and then frozen in an embedding compound (Sakura Finetechnical, Tokyo, Japan). All samples were stored at −30°C until use. The sections were cut transversely at a thickness of 8 μm on a cryostat (Leica CM1510, Leica Microsystems, Heidelberg, Germany). The hippocampus sections were blocked in 5% normal goat serum in 0.01 M phosphate-buffered saline (PBS) for 1 h at room temperature. Each primary antibody was diluted in 0.01 M PBS containing 5% normal goat serum (guinea pig polyclonal antibody to doublecortin [1:3500; Abcam Ltd., Cambridge, UK]), and incubated for two days overnight at 4°C. The samples were then rinsed and incubated with the appropriate secondary antibody conjugated with Alexa 488 for 2 h at room temperature. The slides were then coverslipped with PermaFluor Aqueous mounting medium (Immunon, Pittsburgh, PA). Fluorescence of immunolabeling was detected using a light microscope (Olympus AX-70; Olympus, Tokyo, Japan, and a Radiance 2000 laser-scanning microscope; BioRad, Richmond, CA), and photographed with a digital camera (Polaroid PDMCII/OL; Olympus).

Total RNA in the hippocampus of aged mice was extracted using the SV Total RNA Isolation system (Promega, Madison, WI) following the manufacturer's instructions. Purified total RNA was quantified spectrophotometrically at A_{260}. To prepare first-strand cDNA, 1 μg of RNA was incubated in 100 μl of buffer containing 10 mM dithiothreitol, 2.5 mM $MgCl_2$, dNTP mixture, 50 U of reverse transcriptase II (Invitrogen, Carlsbad, CA), and 0.1 mM oligo-$dT_{12\text{-}18}$ (Invitrogen). Each gene was amplified in 50 μl of PCR solution containing 0.8 mM $MgCl_2$, dNTP mixture, and DNA polymerase with synthesized primers (Table I). Samples were heated to 95°C for 1 min, 55°C for 2 min, and 72°C for 3 min. The final incubation was at 72°C for 7 min. The mixture was run on 2% agarose gel electrophoresis with the indicated markers and primers for the internal standard glyceraldehyde-3-phosphate dehydrogenase. The agarose gel was stained with ethidium bromide and photographed with UV transillumination. The intensity of the bands was analyzed and semiquantified by computer-assisted densitometry using ImageJ software. Values represent the mean ± SEM of three independent experiments.

TABLE I. Comprehensive List of All Primer Sequences Used

Experiment	Name	Sequence
RT-PCR	DCX	F: CTTTTGGTTCAGCAGAAGGG
		R: CAAATGTTCTGGGAGGCACT
	GFAP	F: ACAACTTTGCACAGGACCTC
		R: CGATTCAACCTTTCTCTCCA
	BDNF	F: TCACTGGCTGACACTTTTGAG
		R: CTATCCTTATGAATCGCCAGC
	MLL1	F: AGCGGAGAGGATGAGCAGT
		R: CGAGGTTTTCGAGGACTAGC
	LSD1	F: TCAACGTCCTCAATAATAAACCTGT
		R: CCTGAGTTTTCACTATCTTCTTCCA
	Jaridla	F: CCTCCATTTGCCTGTGAAGT
		R: CCTTTGCTGGCAACAATCTT
	Jaridlb	F: AGAGGCTGAATGAGCTGGAG
		R: TGGCAATTTTGGTCCATTTT
	jmjd2A	F: GACCACACTCTGCCCACAC
		R: TCCTGGGGTATTTCCAGACA
	jmjd2B	F: GGCTTTAACTGCGCTGAGTC
		R: GTGTGGTCCAGCACTGTGAG
	jmjd2C	F: CACGGAGGACATGGATCTCT
		R: CGAAGGGAATGCCATACTTC
	jmjd2D	F: GTCTTGGTCGTCGTCCTTGT
		R: AATCCCCCTTCAGAAGCTGT
	EZH2	F: GCCAGACTGGGAAGAAATCTG
		R: TGTGCTGGAAAATCCAAGTCA
	UTX	F: ATCCCAGCTCAGCAGAAGTT
		R: GGAGGAAAGAAAGCATCACG
	jmjd3	F: CCCCCATTTCAGCTGACTAA
		R: CTGGACCAAGGGGTGTGTT
	GAPDH	F: CCCCACGGCAAGTTCAACGG
		R: CTTTCCAGAGGGCCATCCA
Real-time PCR	DCX	F: CTTTTGGTTCAGCAGAAGGG
		R: CAAATGTTCTGGGAGGCACT
	β-actin	F: CAGCTTCTTTGCAGCTCCTT
		R: TCACCCACATAGGAGTCCTT
ChIP	DCX	F: AGCTTGCCTGTGCAATCTTT
		R: GAACACCCCCAACCTCCTAT

Fast SYBR Green Master Mix (2x) (Applied Biosystems, Inc., CA) was used as the basis for the reaction mixture in the real-time PCR assay. Each gene prepared by the above procedure was amplified in 20 μl of a PCR solution containing 10 μl of the Fast SYBR Green Master Mix (2x) with synthesized primers (Table I). In addition to each sample, each test run included a no-target control that contained reaction mixture and PCR-grade water. PCR with a StepOnePlus™ (Applied Biosystems, Inc., CA) was performed with the following cycling conditions: 95°C for 20 s, followed by 45 cycles of 95°C for 3 s and 60°C for 30 s. Fluorescence detection was conducted after each extension step.

A ChIP assay was performed as described previously (Takeshima et al., 2009; Tsankova et al., 2004) with minor modifications. Briefly, mouse hippocampus tissue was dissected as described above and cross-linked, and then tissue was lysed. Fifteen μg of soluble chromatin was incubated with 2 μg of specific antibodies against acetylated histone H3 (Millipore), H3K4 trimethylation (Wako Pure Chemicals, Osaka, Japan), H3K9 trimethylation (Millipore), H3K27 trimethylation (Millipore), overnight at 4°C. The immunocomplex was collected by Dynabeads Protein A (Invitrogen Dynal AS, Oslo, Norway), and DNA was recovered with RNaseA treatment, Proteinase K treatment followed by isopropanol precipitation. Immunoprecipitated DNA was dissolved in 50 μl of 1 × TE and 1 μl was used for quantitative PCR. Quantitative PCR was performed as described previously (Nakajima et al., 2009). The primers used are listed in Table I.

The data are expressed as the mean ± S.E.M. The statistical significance of differences between groups was assessed with Student's *t*-test (comparison of two groups) or an analysis of variance (ANOVA) followed by the Bonferroni test (comparison among multiple groups). A level of probability of 0.05 or less was considered significant.

Doublecortin is a cytoskeletal protein that is transiently expressed only in newborn neurons, and is used as a marker of neural progenitors. In agreement with a previous report (Hwang et al., 2008), we confirmed that doublecortin-positive cells were almost completely absent from the dentate gyrus of the hippocampus of 28-month-old mice (Fig. 1A). The level of doublecortin, the doublecortin mRNA was significantly decreased in the hippocampus of aged mice compared to that in young mice (Figs. 1B and 1C, $P < 0.001$ vs. young mice). In contrast, mRNA levels of glial fibrillary acidic protein (GFAP), a glial marker, and brain-derived neurotrophic factor (BDNF) in the hippocampus were not altered by normal aging.

We next evaluated whether changes in doublecortin mRNA expression accompanied by aging could be regulated through chromatin-specific events. In this study, we analyzed two active histone modifications (acetylation of histone H3, AcH3, and trimethylation of lysine 4 on histone H3, H3K4) and two repressive histone modifications (trimethylation of lysine 9 on histone H3, H3K9, and trimethylation of lysine 27 on histone H3, H3K27) at doublecortin promoter regions in the hippocampus. As a result, we detected a significant decrease in H3K4 trimethylation at the doublecortin promoters with aging (Fig. 2A, $P < 0.05$ vs. young mice). Furthermore, a significant increase in H3K27 trimethylation at the doublecortin gene was seen with aging (Fig. 2A, $P < 0.05$ vs. young mice). Under these conditions, aging did not produce H3K9 trimethylation or hyperacetylation of H3 at the doublecortin gene (Fig. 2A).

The methylation of H3K9 and H3K27 can be directly modulated by histone methylases and demethylases that target specific lysine residues and methylation states. Thus, we finally investigated whether aging could alter the mRNA level of several histone methylases and demethylases in the hippocampus. We found that aging did not change the mRNA expression of MLL1 (a H3K4 methyltransferase), LSD1, Jarid1a or Jarid1b (H3K4 demethylases), jmjd2A, jmjd2B, jmjd2C or jmjd2D (H3K9 demethylases), EZH2 (a H3K27 methyltransferase), or UTX or jmjd3 (H3K27 demethylases) (Fig. 2B).

Doublecortin is a microtubule-associated protein that is expressed specifically in virtually all migrating neural precursors of the CNS and has been used as a candidate marker for neuronal migration and differentiation. In this study, aging caused a dramatic decrease in levels of doublecortin mRNA in the hippocampus. In the dentate gyrus of the hippocampus, few or no doublecortin-positive cells were observed by aging. These findings strongly suggest that an aging can stimulate the impairment of neuronal differentiation from precursors in the hippocampal dentate gyrus. These notions are supported by previous reports that aging promoted the impairment of neurogenesis (Kuhn et al., 1996; Lichtenwalner et al., 2001).

Epigenetic alterations of DNA play key roles in determining gene structure and expression (Jaenisch and Bird, 2003; Tsankova et al., 2007). A major epigenetic modification, chromatin remodeling, modulates gene expression with high temporal and spatial resolution by permitting small groups of nucleosomes to become more or less open, which consequently enhances or inhibits access of the transcriptional machinery to specific promoter regions. The acetylation and methylation of histone proteins at specific residues play a major role in chromatin remodeling. Lysine acetylation almost always correlates with chromatin accessibility and transcriptional activity, whereas lysine methylation can have different effects depending on which residue is modified. Trimethylation of H3K4

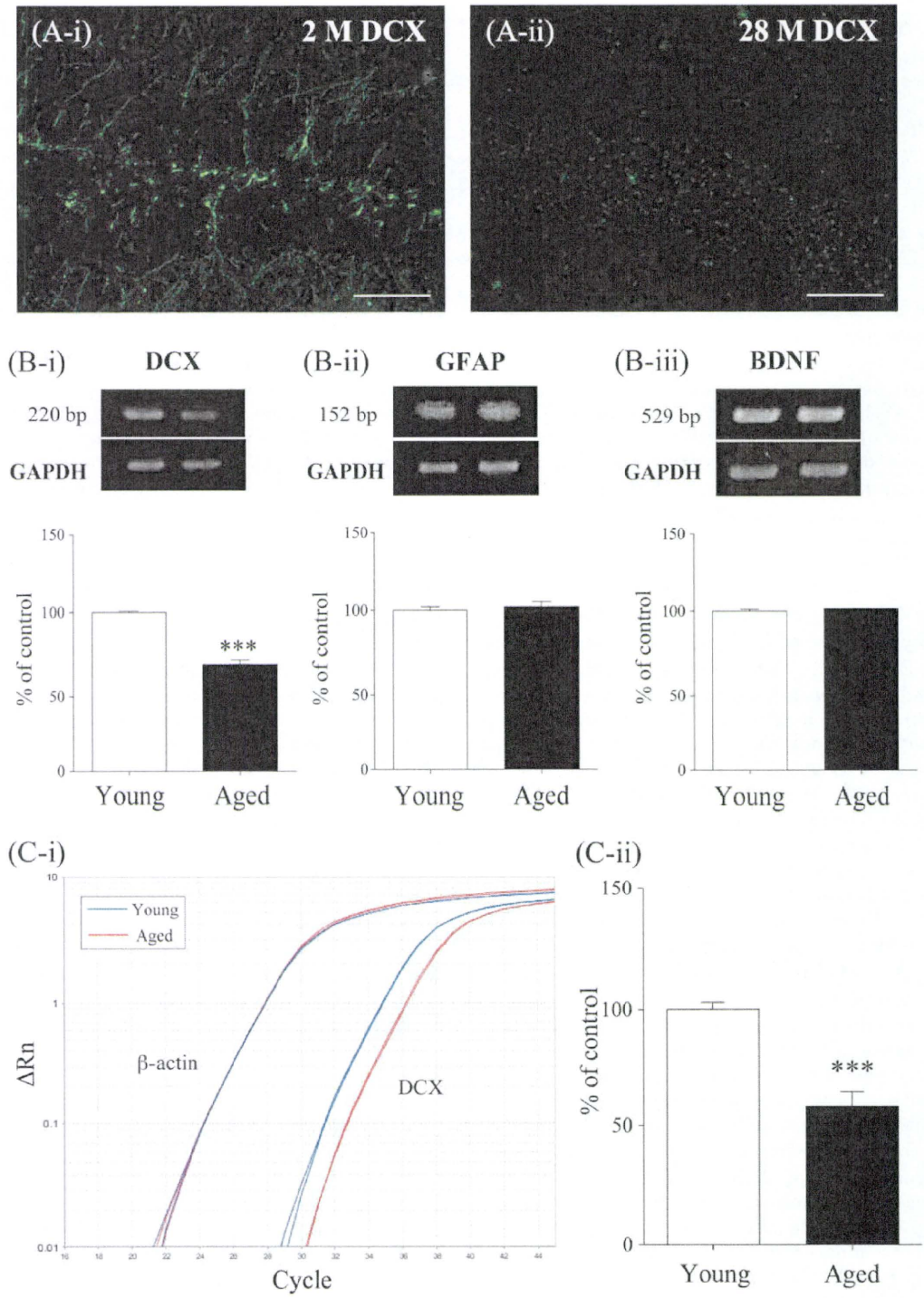

Fig. 1. (**A**) Immunofluorescent staining for doublecortin in the dentate gyrus in young and aged mice. Doublecortin-like immunoreactivity in the dentate gyrus of 28-month-old mice (A-ii) was decreased compared to that in 2-month-old mice (A-i). Scale bar: 50 μm. (**B**) Upper: Representative RT-PCR for doublecortin (DCX; B-i), GFAP (B-ii) and BDNF (B-iii) mRNAs in the hippocampus obtained from young and aged mice. Lower: The intensity of the bands was semiquantified using NIH Image software. The values for DCX, GFAP and BDNF mRNA were normalized by that for the internal standard glyceraldehyde-3-phosphate dehydrogenase (GAPDH) mRNA. The value for aged mice is expressed as a percentage of the increase in young mice. Each column represents the mean ± S.E.M. six samples. $^{***}P < 0.001$ vs. the young group. (**C**) Quantitative analysis of DCX mRNA in the hippocampus obtained from young and aged mice. (C-i) Amplification plots of fluorescence intensities vs. PCR cycle numbers in each sample. (C-ii) Each column represents the mean ± S.E.M. of three samples. $^{***}P < 0.001$ vs. the young group.

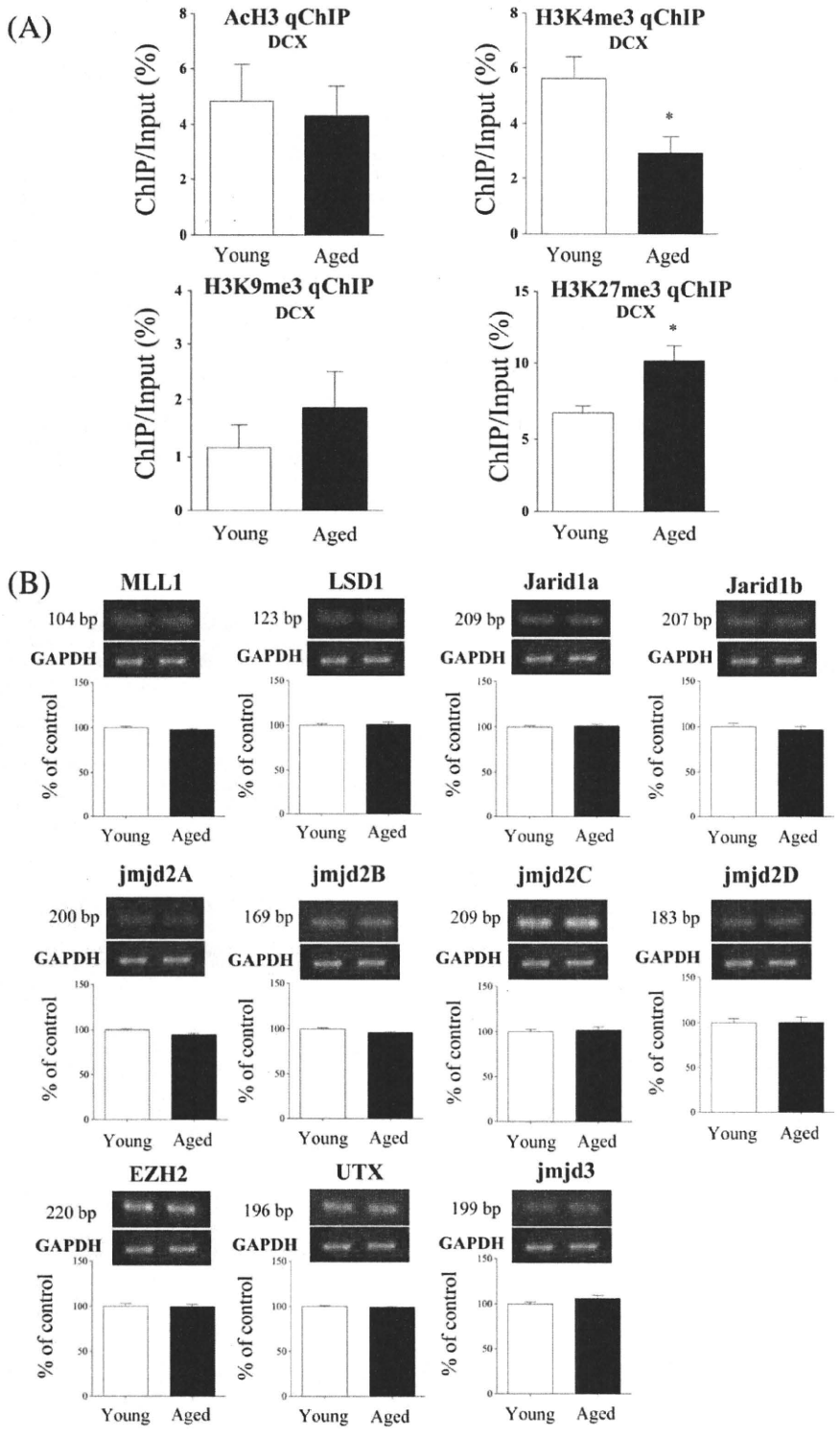

Fig. 2. **A**: Stable changes in histone modifications in the hippocampus in aged mice. ChIP assays were performed to measure the levels of several histone modifications at the doublecortin (DCX) promoter in the hippocampus using specific antibodies for each modification state. Levels of promoter enrichment were quantified by quantitative PCR. Histone H3 was not altered at DCX. Significant changes in acetylation (AcH3) or H3K9 trimethylation (H3K9me3) were not detected at the DCX promoter region. Histone H3K4 trimethylation (H3K4me3) was decreased at the DCX promoter region in aged mice. $^*P < 0.05$ vs. the young group. Histone H3K27 trimethylation (H3K27me3) was increased at the DCX promoter region in aged mice. $^*P < 0.05$ vs. the young group. **B**: Upper: Representative RT-PCR for MLL1 (a H3K4 methyltransferase), LSD1, Jarid1a and Jarid1b (H3K4 demethylases), jmjd2A, jmjd2B, jmjd2C and jmjd2D (H3K9 demethylases), and EZH2 (a H3K27 methyltransferase), and UTX and jmjd3 (H3K27 demethylases). mRNAs in the hippocampus obtained from young and aged mice. Lower: The intensity of the bands was semiquantified using NIH Image software. The value for mRNA was normalized by that for the internal standard glyceraldehyde-3-phosphate dehydrogenase (GAPDH) mRNA. The value for aged mice is expressed as a percentage of the increase in young mice. Each column represents the mean ± S.E.M. of six samples.

is associated with transcribed chromatin. In contrast, trimethylation of H3K9 and H3K27 generally correlates with repression (Bernstein et al., 2007). In agreement with the PCR assay, we found here that aging caused a significant decrease in H3K4 trimethylation and a significant increase in H3K27 trimethylation at the doublecortin gene. In contrast, we failed to find any changes in the H3K9 trimethylation and hyperacetylation of H3 at the doublecortin gene. These findings suggest that aging produces a dramatic decrease in the expression of the neuronal progenitor doublecortin along with epigenetic modifications in the hippocampus.

Histone methylation is dynamically regulated by a plethora of methylases and demethylases (Swigut and Wysocka, 2007). In the present study, aging failed to change the mRNA expression of several methylases and demethylases including MLL1 (a H3K4 methyltransferase), LSD1, Jarid1a and Jarid1b (H3K4 demethylases), jmjd2A, jmjd2B, jmjd2C and jmjd2D (H3K9 demethylases), EZH2 (a H3K27 methyltransferase), and UTX and jmjd3 (H3K27 demethylases). These findings suggest that aging causes a dramatic decrease in neurogenesis accompanied by epigenetic modification related to the decreased expression of doublecortin without changing the expression of their associated histone methylases and demethylases in the hippocampus.

In conclusion, although further investigation is still required, the present findings suggest that decreased expression of the migrated neural progenitor doublecortin associated with histone modification may be, at least in part, involved in an aging-dependent decrease in neurogenesis in the hippocampus. Since the methylation of H3K27 is especially considered to play a critical role in the long-lasting silencing of targeted gene expression (Swigut and Wysocka, 2007), the present finding of the epigenetically repressive modulation of neural progenitors could allow us to better understand the mechanism of aging-dependent hippocampal dysfunction.

REFERENCES

Barnes CA. 1994. Normal aging: Regionally specific changes in hippocampal synaptic transmission. Trends Neurosci 17:13–18.

Bernstein BE, Meissner A, Lander ES. 2007. The mammalian epigenome. Cell 128:669–681.

Bliss TV, Collingridge GL. 1993. A synaptic model of memory: Long-term potentiation in the hippocampus. Nature 361:31–39.

Eriksson PS, Perfilieva E, Bjork-Eriksson T, Alborn AM, Nordborg C, Peterson DA, Gage FH. 1998. Neurogenesis in the adult human hippocampus. Nat Med 4:1313–1317.

Geinisman Y, DeToledo-Morrell L, Morrell F, Persina IS, Rossi M. 1992. Age-related loss of axospinous synapses formed by two afferent systems in the rat dentate gyrus as revealed by the unbiased stereological dissector technique. Hippocampus 2:437–444.

Gravina S, Vijg J. 2009. Epigenetic factors in aging and longevity. Pflugers Arch (in press).

Hwang IK, Yoo KY, Yi SS, Kwon YG, Ahn YK, Seong JK, Lee IS, Yoon YS, Won MH. 2008. Age-related differentiation in newly generated DCX immunoreactive neurons in the subgranular zone of the gerbil dentate gyrus. Neurochem Res 33:867–872.

Jaenisch R, Bird A. 2003. Epigenetic regulation of gene expression: How the genome integrates intrinsic and environmental signals. Nat Genet 33 (Suppl):245–254.

Kempermann G, Kuhn HG, Gage FH. 1997. More hippocampal neurons in adult mice living in an enriched environment. Nature 386: 493–495.

Kuhn HG, Dickinson-Anson H, Gage FH. 1996. Neurogenesis in the dentate gyrus of the adult rat: Age-related decrease of neuronal progenitor proliferation. J Neurosci 16:2027–2033.

Lichtenwalner RJ, Forbes ME, Bennett SA, Lynch CD, Sonntag WE, Riddle DR. 2001. Intracerebroventricular infusion of insulin-like growth factor-I ameliorates the age-related decline in hippocampal neurogenesis. Neuroscience 107:603–613.

Lois C, Alvarez-Buylla A. 1993. Proliferating subventricular zone cells in the adult mammalian forebrain can differentiate into neurons and glia. Proc Natl Acad Sci USA 90:2074–2077.

Nakajima T, Yamashita S, Maekita T, Niwa T, Nakazawa K, Ushijima T. 2009. The presence of a methylation fingerprint of *Helicobacter pylori* infection in human gastric mucosae. Int J Cancer 124:905–910.

Swigut T, Wysocka J. 2007. H3K27 demethylases, at long last. Cell 131:29–32.

Takeshima H, Yamashita S, Shimazu T, Niwa T, Ushijima T. 2009. The presence of RNA polymerase II, active or stalled, predicts epigenetic fate of promoter CpG islands. Genome Res 19:1974–1982.

Tsankova NM, Kumar A, Nestler EJ. 2004. Histone modifications at gene promoter regions in rat hippocampus after acute and chronic electroconvulsive seizures. J Neurosci 24:5603–5610.

Tsankova N, Renthal W, Kumar A, Nestler EJ. 2007. Epigenetic regulation in psychiatric disorders. Nat Rev Neurosci 8:355–367.

van Praag H, Kempermann G, Gage FH. 1999. Running increases cell proliferation and neurogenesis in the adult mouse dentate gyrus. Nat Neurosci 2:266–270.

Molecular analysis of single isolated glands in gastric cancers and their surrounding gastric intestinal metaplastic mucosa

TAMOTSU SUGAI[1], WATARU HABANO[2], YU-FEI JIAO[1], MINORU TOYOTA[3], HIROMU SUZUKI[3], MITSUNORI TSUKAHARA[1,4], HITOHIKO KOIZUKA[1,4], RISABURO AKASAKA[1,4], KEISUKE KOEDA[5], GO WAKABAYASHI[5] and KAZUYUKI SUZUKI[4]

[1]Department of Pathology, Division of Diagnostic Molecular Pathology, School of Medicine, [2]Department of Pharmacodynamics and Molecular Genetics, School of Pharmacy, Iwate Medical University, Iwate; [3]Department of Biochemistry, School of Medicine, Sapporo Medical University, Sapporo; [4]Department of Internal Medicine, Division of Gastroenterology and Hepatology, [5]Department of Surgery, School of Medicine, Iwate Medical University, Iwate, Japan

Received June 9, 2009; Accepted August 7, 2009

DOI: 10.3892/or_00000602

Abstract. The biological properties and underlying genetics of gastric cancer and gastric intestinal metaplasia evolve with neoplastic progression from the genetics of the original gland cell. PCR assay with crypt isolation was used in tumors from 20 patients to examine microsatellite alterations (allelic imbalance at 17p, 5q, 18q, 3p, 4p, and 9p, and microsatellite instability) in glands from each tumor and from intestinal metaplastic lesions. Tumor specimens were processed as either pooled-gland samples or single-gland samples. Pooled gland sample was composed of 10-20 tumor glands, intestinal metaplastic glands, or nonmetaplastic glands. Single gland sample was 10 tumor glands from tumor and single gland sample was 5 gastric intestinal metaplastic and 5 nonmetaplastic glands from its surrounding metaplastic mucosa. Multiple genetic alterations were found in individual tumor glands, with various subclonal expansions seen within the same tumor. Although microsatellite instability was found in 2 of 20 tumor single-gland samples, none was detected in metaplastic single-gland samples. Most cancers appear to have a heterogeneous composition. On the other hand, microsatellite alterations were also detected within the nonmetaplastic as well as intestinal metaplastic single-gland samples. In conclusion, the present data on tumor and corresponding intestinal metaplastic and nonmetaplastic glands suggest that genetic alterations already occur within the surrounding of the noncancerous mucosa.

Correspondence to: Dr Tamotsu Sugai, Division of Diagnostic Molecular Pathology, Department of Pathology, 19-1 Morioka, Iwate 020-8505, Japan
E-mail: tsugai@cocoa.ocn.ne.jp

Key words: crypt isolation, gastric cancer, intestinal metaplasia, loss of heterozygosity, microsatellite instability

Introduction

It has long been established that gastric cancers develop from a single gland cell that undergoes an accumulation of genetic changes (1), and which eventually results in a malignant tumor with monoclonal character (2,3). Recent molecular genetic evidence also supports this concept (1). Despite the monoclonal origin of such cancerous tumors, any single tumor consists of numerous tumor glands, which may have various genetic alterations relative to the cell of origin. According to established theory, these accumulated genetic alterations can be identified by loss of heterozygosity (LOH) at many chromosomal loci within the tumor (4). It is also true that differences between tumor glands are thought to cause genetic heterogeneity within the same tumor (1-3), and some studies stated that genetic heterogeneity is frequently found in individual gastric cancers (5-7). Such genetic heterogeneity within the same tumor complicates the development of a tumor-treatment strategy based on tumor pathogenesis (8,9). Analyzing the accumulation of multiple genetic alterations in a single tumor gland is thought to be useful for assessing genetic differences among the cells of a single tumor (2,3).

Gastric intestinal metaplasia (GIM) is frequently found in the mucosa surrounding a gastric cancer (10), and is commonly thought to be a precancerous condition for gastric cancer, especially differentiated-type gastric cancers (11,12). However, an alternative hypothesis, the 'paracancerous' condition, as distinct from the 'precancerous' condition, has been described, especially in Japan (13). The paracancerous hypothesis derives from the fact that, based on routine pathological examination of surgical specimens, no pathologist has yet been able to identify the feature proving that differentiated-type gastric carcinomas arise directly from intestinal metaplastic glands. Accordingly, it remains unclear whether GIM is truly a precancerous lesion. In addition, GIM is not a single entity but rather a heterogeneous group of metaplastic glands (14). Previous studies suggested that GIM by itself is associated with carcinogenesis of differentiated-type gastric cancer and that GIM has a heterogeneous composition with different

biological characteristics (14-17). Identification of 1 or more biomarkers to reliably differentiate GIM types associated with gastric cancer and the molecular alterations associated with various types of GIM may be very valuable clinically as a tool for identifying patients who may be at higher risk for gastric cancer. However, molecular alterations contributing to the development or neoplastic progression of GIM have not been clarified (18). In addition, a non-neoplastic gland which is seen in the gastric intestinal metaplastic mucosa is not necessarily an intestinal metaplastic gland. Nonmetaplastic glands are often observed in gastric metaplastic mucosa. It is likely that the nonmetaplastic glands are also associated with gastric carcinogenesis. However, the molecular alterations of nonmetaplastic glands within the gastric intestinal metaplastic mucosa are still not identified.

For genetic evaluations of an individual gland taken from tissue of a single gastric cancer and the surrounding GIM and nonmetaplastic glands (intestinal metaplastic and non-intestinal glands), it is necessary to isolate single glands from the larger tissue mass. The crypt isolation method can be used to obtain individual tumor and non-neoplastic glands from a given tumor or surrounding tissue (19,20). In the current study, we used crypt isolation methodology to examine molecular alterations of single tumor glands from a gastric cancer and single glands from surrounding GIM tissue. The aim of this study was to verify the role of intratumoral molecular differences in sporadic gastric cancer and to further our understanding of molecular alterations in GIM tissue that result in gastric tumorigenesis.

Materials and methods

Tissue samples. Tissues were obtained from 20 patients with sporadic primary gastric adenocarcinoma of differentiated type, who had undergone gastrectomy. Of the 20 patients, there were 17 men and 3 women (mean age: 64.2 years). Tumor histological type and stage were classified according to the Japanese Research Society criteria for cancer of the stomach (21). The location of the gastric cancer was determined and the tumors were subclassified into 2 groups: proximal or distal. Clinicopathological data for the 20 patients in our study are shown in Table I. In addition, in order to clarify genetic alterations in non-neoplastic glands not demonstrating intestinal metaplasia (nonmetaplastic gland), nonmetaplastic glands associated with gastric adenocarcinomas were analyzed in the 10 tumors in which they were available.

Fresh tumor specimens and adjacent tissue were obtained from resected gastric cancers. Gastric mucosa most distal to the tumor that was regarded as normal was removed from the submucosa with scissors and discarded. In contrast, intestinal metaplastic mucosa was obtained from antral mucosa. Tissue tumor samples were obtained primarily from the central area of the tumor.

Crypt isolation technique. Isolation of tumor and mucosal glands was performed as previously described (22). Briefly, fresh tumor and non-neoplastic mucosa were separated from the underlying tissue layer and cut with a razor into minute pieces, and then incubated at 37°C for 30 min in Hanks' balanced salt solution (HBSS), which is calcium- and magnesium-free, containing 30 mmol/l ethylenediaminetetraacetic acid (EDTA). Specimens were stirred in HBSS for 30-40 min to allow isolation of cancerous and normal glands from the lamina propria mucosa or fibrous stroma. Isolated specimens were immediately fixed in 70% ethanol and stored at 4°C until analysis.

Table I. Clinicopathological findings of gastric cancers examined.

Total	20
Gender (male/female)	17/3
Age (mean)	32-80 (62.7)
Locus	
Proximal	2
Distal	18
Histological type	
WDA	8
MDA	12
Stage	
I	3
II	4
III	10
IV	3

WDA, well differentiated adenocarcinoma; MDA, moderately differentiated adenocarcinoma.

Representative cancerous glands are shown in Fig. 1a-f. To obtain intestinal metaplastic glands, nonmetaplastic glands were isolated from antral mucosa [stained with Alcian blue (pH 2.5).

Identification of isolated gastric intestinal metaplastic glands. In the present study, GIM was recognized by the presence of goblet cells stained by Alcian blue. Detailed histological identification of intestinal metaplasia was performed on sections of paraffin-embedded tissue located adjacent to the tissue used for crypt isolation. Most tissue sections showed incomplete intestinal metaplasia.

Identification of isolated gastric intestinal nonmetaplastic glands. Nonmetaplastic glands which were not stained by Alcian blue were isolated from antral mucosa. These glands could be easily distinguished from metaplastic glands. However, nonmetaplastic glands were obtainable in only 10 of 20 cases.

Identification of isolated normal gastric glands. Normal mucosal tissue was defined as glands obtained from Alcian blue-negative fundic mucosa, and was confirmed by histological examination. Normal mucosa was used to examine microsatellite alterations in normal (negative) controls.

DNA extraction. Isolated tumor glands were handled as follows: Ten to 20 isolated glands (tumor, intestinal metaplastic, and nonmetaplastic glands) were obtained from each

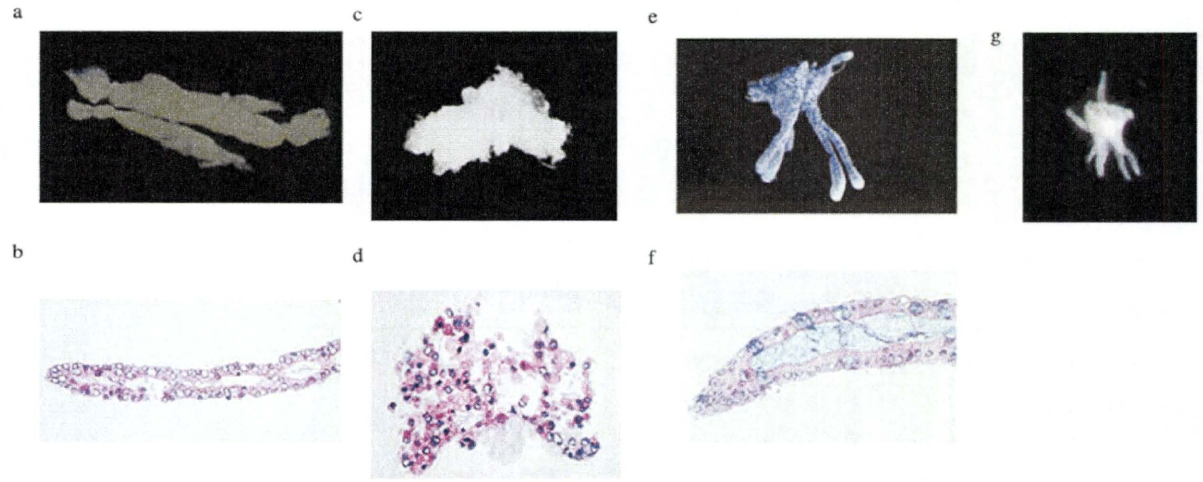

Figure 1. Well-differentiated adenocarcinoma. (a) As seen under a dissecting microscope and (b) with hematoxylin and eosin staining (H&E). A single moderately differentiated tumor gland (c) under a dissecting microscope and (d) as seen with H&E staining. Single intestinal metaplastic gland (e) as stained by Alcian blue (pH 2.5) under a dissecting microscope and visualized with H&E staining (f). Single non-intestinal metaplastic gland (g).

Table II. Frequencies of allelic imbalances at each locus in tumor pooled-gland samples.

	Informative cases	Pooled-gland sample (%)
17p	15	8 (53.3)
5q	18	10 (55.6)
18q	18	8 (44.4)
3p	18	8 (44.4)
4p	18	10 (55.6)
9p	14	13 (92.6)

tissue sample. DNA extraction was performed on these glands to create the pooled-gland samples (3). Separately, 10 tumor glands and 5 intestinal metaplastic glands or nonmetaplastic glands were obtained from each tumor examined and its surrounding antral mucosa. DNA was extracted from each individual tumor, intestinal metaplastic, and nonmetaplastic gland, respectively, to create the single-gland samples, using techniques described previously (2,3). The DNA concentration of single tumor glands was estimated by the TagMan real-time PCR method using the ribosomal protein P0 (3684) gene as a reference (3). In addition, the amount of DNA content that we examined varied from 98.6 to 1034.8 ng (mean: 410.1 ng). On the other hand, that of DNA content examined in single intestinal metaplastic glands varied from 112.6 to 253.4 ng (mean: 198.7 ng).

Microsatellite analysis. Microsatellite analysis included 15 microsatellite markers (2 mono- and 13 dinucleotide repeats). These markers were selected either because of their location at chromosomal sites in or near genes known to be involved in gastric carcinogenesis (3p, 4p, 5q, 9p, 17p, and 18q), or because they are very sensitive markers for determination of microsatellite instability (MSI) (BAT25 and 26). The markers used for analysis of LOH in this study were: 3p (D3S2402, D3S1234), 4p (D4S2639, D4S1601), 5q (D5S107, D5S346, D5S299, D5S82), 9q (D9S171, D9S1118), 17p (TP53), and 18q (D18S487, D18S34).

PCR reactions were performed as described previously (23,24). One of the primers used for amplification was fluorescently labeled. PCR products were separated and detected with an automated sequencing system as previously reported (19,23).

Scoring of allelic imbalance. Allelic imbalance (AI) was determined using a calculation method described previously (25). A tumor was considered to have AI if the allelic peak ratio was <0.6, representing an allelic signal reduction of at least 40%. We interpreted this allelic imbalance as LOH with the provision that, in some cases, the change in allele peak ratio may have resulted from allelic amplification. When AI was observed in at least 1 locus of the markers examined, imbalances of the examined loci were confirmed. Finally, tumors exhibiting MSI at a given locus were not evaluated for LOH.

The overall extent of LOH for each single-gland sample (tumor, intestinal metaplastic, or nonmetaplastic single-gland sample) was calculated as follows: the number of single glands showing LOH divided by the number of informative (excluding uninformative cases, samples showing MSI, and cases that were not examined) single glands for each tumor or each intestinal metaplastic gland sample.

Scoring of microsatellite instability. An additional peak in tumor DNA compared with nontumor tissue was classified as instability for the marker examined. Instability in BAT 25 or 26 was defined as MSI positive (26).

Results

In the present study, PCR analysis was performed reproducibly and there were no PCR failures, as has been described elsewhere (3). The frequencies of allelic imbalance at the

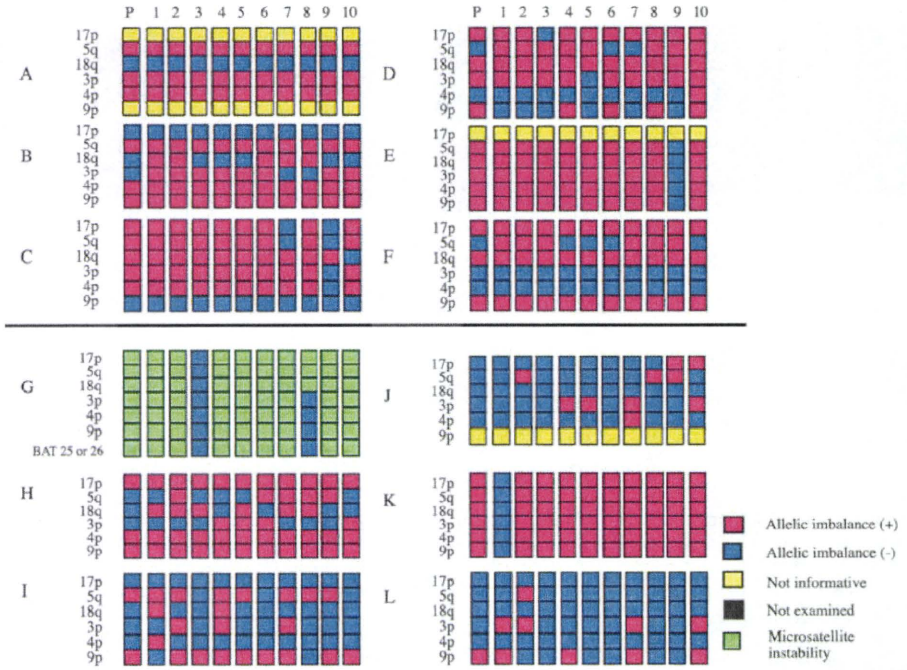

Figure 2. A detailed view of allelic imbalances on 5q, 17p, 18q, 3p, 4p, 9p, and microsatellite instability in pooled-tumor samples and in corresponding tumor single-gland samples (cases: A-L). P, pooled gland sample; LOH, loss of heterozygosity; N, negative; NI, not informative; NA, not amplified; MSI, microsatellite instability.

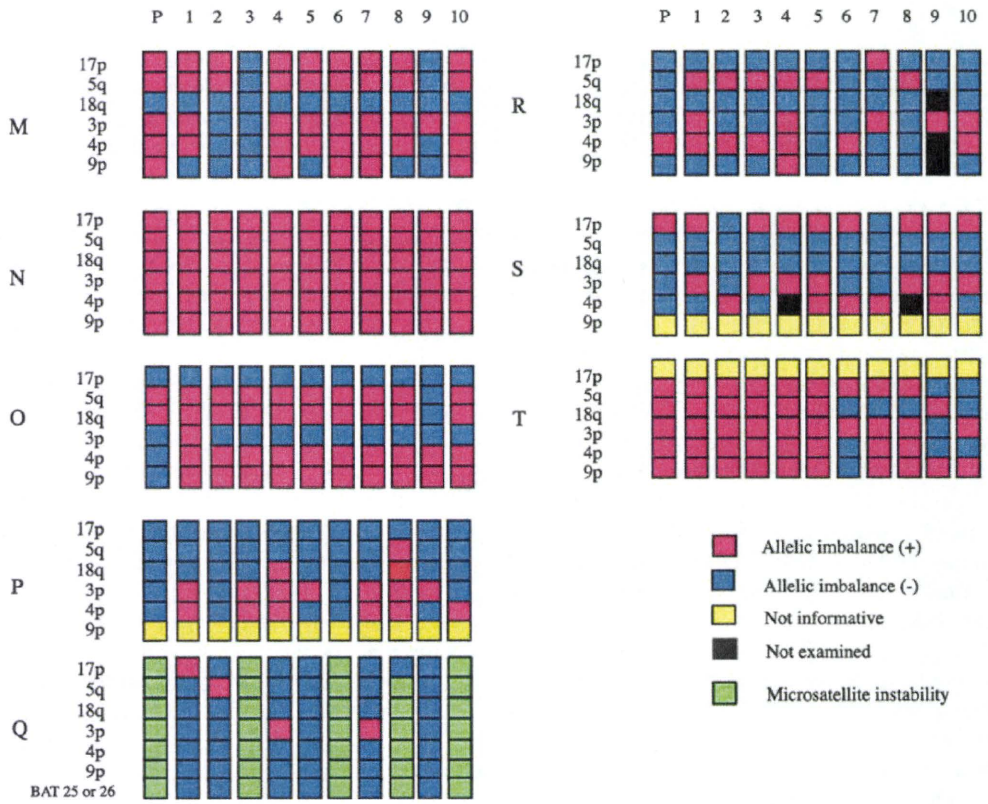

Figure 3. A detailed view of allelic imbalances on 5q, 17p, 18q, 3p, 4p, 9p, and microsatellite instability (MSI) in pooled-tumor samples and in corresponding tumor single-gland samples (cases: M-T). P, pooled gland sample; LOH, loss of heterozygosity; N, negative; NI, not informative; NA, not amplified; MSI, microsatellite instability.

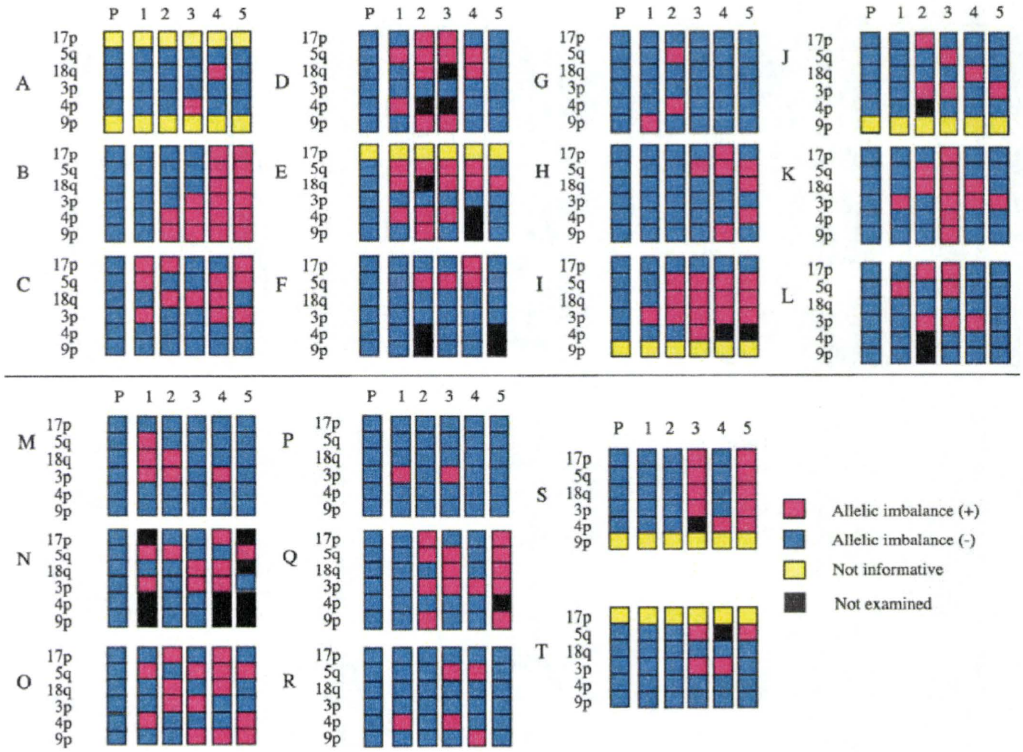

Figure 4. A detailed view of allelic imbalances on 5q, 17p, 18q, 3p, 4p, 9p, and microsatellite instability in intestinal metaplastic pooled-gland samples and in corresponding intestinal metaplastic single-gland samples (samples: A-T). Multiple genetic alterations were seen in the single intestinal metaplastic gland samples. P, pooled gland sample; LOH, loss of heterozygosity; N, negative; NI, not informative; NA, not amplified.

chromosomal loci that were studied in the tumor pooled-gland samples are listed in Table II. We defined genotype as the AI pattern of each examined sample.

Concordance of genotype of pooled-gland samples and single-gland samples. We examined the genotype concordance of pooled-gland samples and the predominant genotype in corresponding single-gland samples. In 4 cases there were different AI patterns seen in the tumor pooled-gland samples and in those of the corresponding tumor single-gland samples (samples B, H, O, and S; Figs. 2 and 3). In addition, in another 7 cases (samples D, F, I, J, L, P, and R; Figs. 2 and 3), the predominant genotypes in tumor single-gland samples were different from those of the corresponding pooled-gland samples. Alternatively, in the other 9 cases the genotypes of the tumor pooled-gland samples were consistent with those of the corresponding tumor single-gland samples (Figs. 2 and 3).

In the samples of intestinal metaplastic glands, although no genetic alterations were found in the pooled-gland samples, multiple alterations were frequently detected in single-gland samples (Fig. 4). A representative example of allelic imbalance at each chromosomal locus in a pooled-gland sample and in corresponding intestinal metaplastic single-gland samples is illustrated in Fig. 5 (case C).

In the samples of nonmetaplastic glands, although no genetic alterations were found in the pooled-gland samples, alterations were observed in corresponding single-gland samples (Fig. 6).

Heterogeneous genotypes in individual glands within the same sample. A total of 18 carcinomas (18/20, 90%) consisted of heterogeneous single genotypes (>1 different genotype) within the same tumor. Single glands within the same sample having the same genotype were interpreted as an occurrence of the same subclone. The number of subclones within the same sample was determined and is shown in Table III. Many subclones were identified within the same sample. No more than 7 different genotypes (subclones) in single-tumor glands from the same sample were observed. In addition, multiple subclones within the same sample of not only intestinal metaplastic single glands but also nonmetaplastic single glands were found. The mean numbers of genetic alterations per tumor, intestinal metaplastic, and nonmetaplastic single-gland samples were 4.15, 3.75 and 4.5, respectively.

Two samples (10%) had homogeneous single genotypes within the same tumor (A and N, Figs. 2 and 3). In contrast, MSI did not occur in a homogeneous pattern within the same tumor (G and Q, Figs. 2 and 3). There were no homogeneous patterns observed among either metaplastic or nonmetaplastic single-gland samples (Figs. 4 and 6).

Genotypic pattern of individual glands within the same sample. As shown in our previous study on colorectal carcinoma (3), the genotype of each single-tumor gland was classified as either a major-altered or a minor-altered genotype. The first group, the major-altered genotype, was defined as a single-tumor gland with >1 genetic alteration. In contrast, the minor-altered genotype was defined as a single-tumor gland with none or

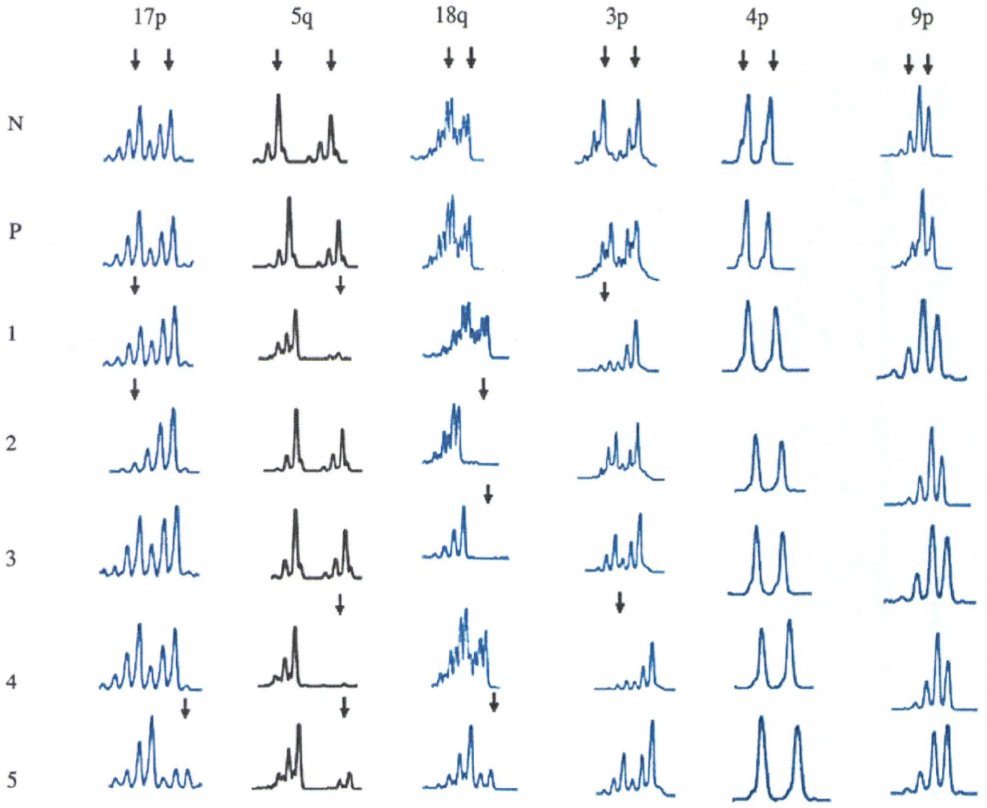

Figure 5. Allelic imbalances on 17p, 5q, 18q, 3p, 4p, and 9p chromosomal loci in an intestinal metaplastic pooled-gland sample and in corresponding intestinal metaplastic single-gland samples (case C). Multiple subclones (genotypes) were seen. Note that although no genetic alterations were detected in the pooled-gland sample, they were frequently found in the paired single intestinal metaplastic gland sample. In intestinal metaplastic single-gland samples, arrows indicate a lost allele at each chromosomal locus. P, pooled gland sample; N, normal.

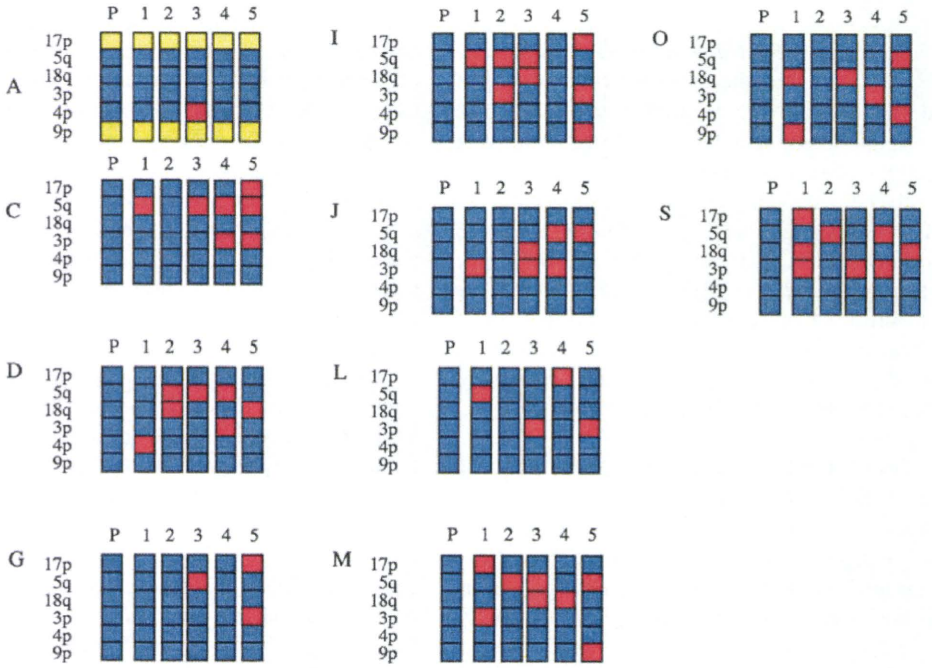

Figure 6. A detailed view of allelic imbalances on 5q, 17p, 18q, 3p, 4p, 9p, and microsatellite instability in nonmetaplastic pooled-gland samples and in corresponding nonmetaplastic single-gland samples (cases: A, C, D, G, I, J, L, M, O, and S). Genetic alterations were seen in the single intestinal metaplastic gland samples. The frequency of allelic imbalances in single nonmetaplastic gland samples is low compared with those of single intestinal metaplastic gland samples. P, pooled gland sample; LOH, loss of heterozygosity; N, negative; NI, not informative; NA, not amplified.

Table III. The number of subclones within the same sample.

Number of subclones within the same tumor	Number of cases		
	Tumor gland	Intestinal metaplastic gland	Nonmetaplastic gland
Two	3	2	1
Three	3	6	1
Four	3	7	3
Five	2	5	5
Six	5	0	0
Seven	2	0	0

with 1 genetic alteration. The major-altered genotype contained 2 types of genetic alterations: multiple AI (AI-type) and MSI. Of 20 carcinomas, 12 contained single-tumor glands with the minor-altered genotype within the same tumor. In contrast, all samples of intestinal metaplastic single glands contained the minor-altered genotype with the exception of one case (sample O). However, surprisingly, at least 1 metaplastic single gland with the major-altered genotype metaplastic glands was detected in 18 of 20 samples. Among the nonmetaplastic single-gland samples, there were major-altered genotypes found in 8 of 10 samples.

Classification of genotype alterations in a single gland within individual tumor. Similar to our previous study (3), we categorized the samples we examined (gastric cancers, intestinal metaplastic glands, nonmetaplastic glands, and including homogeneous tumors) into 5 groups according to criteria based on proportion of genotype alteration: I, all major-altered genotypes; II, major-altered > minor-altered genotypes; III, major-altered = minor-altered genotypes; IV, minor-altered > major-altered genotypes; V, all minor-altered genotypes. According to these criteria, of single glands from tumors, 8 samples were categorized as type I, 8 as type II, and 3 tumors as type IV. The remaining tumor was classified as type III. No tumor was type V. The 2 tumor samples with MSI were grouped as type II and IV, respectively. In contrast, among samples of intestinal metaplastic single glands, 1 was classified as type I, and 9 and 8 samples were categorized as type II and IV, respectively. Two samples were classified as type V. Among nonmetaplastic gland samples, 2 were classified as type II, 2 as types V, and 6 as type IV.

We looked for any association between the genotypes of pooled-gland samples (major-altered and minor-altered genotypes) and the genotypic patterns (I-V) of tumor, intestinal metaplastic, and nonmetaplastic single-gland samples; results are shown in Table IV. In 3 tumor samples (Q, R, and S), the genotype in pooled-gland samples was not consistent with the genotypic patterns of tumor single-gland samples. In contrast, in 10 intestinal metaplastic samples (B, C, D, E, I, J, K, N, O, and Q), the genotype of pooled-gland samples in GIM was different from the genotypic patterns of intestinal metaplastic single-gland samples. In addition, in 7 nonmetaplastic samples (C, D, I, J, M, O, and S), the genotype of pooled-gland samples in nonmetaplastic glands was not consistent with the genotype pattern of nonmetaplastic single-gland samples.

Discussion

In the present study, 12 of 20 tumors showed different predominant genotypes between pooled-gland and single-gland tumor samples. These 12 tumors were primarily classified into 2 groups as an explanation of the discrepancy between pooled-gland and single-tumor gland samples (3). The first explanation is that the AIs in pooled-gland samples at the chromosomal loci we examined may be caused by dilution of minor genotypes within the same tumor (dilution effect). This may represent a mean value of AIs for all collected single-gland tumors. We concluded that the results for 4 tumors (samples: F, I, J, and L) are consistent with this explanation. An alternative explanation may be that the composition of tumor glands in the pooled-gland samples is different from that observed in the single-gland tumor sample (i.e., different composition effect). This suggests that additional subclones, different from those found in the pooled-gland tumor sample, can exist within the same tumor. According to this explanation, it may be likely that a different subclone or different composition of a single-gland sample will not be detected in the pooled-gland samples (B, D, H, O, P, Q, R, and S).

Such a discrepancy between pooled-gland and single-gland samples was prominent in the nonmetaplastic samples. Although no genetic alterations were detected in the pooled-gland samples, multiple genetic alterations were found in corresponding single-gland samples. In particular, this finding was frequently present in GIM samples.

In the present study, it appears that isolation of single intestinal metaplastic glands can be used to increase the sensitivity of tests for allelic imbalance. This finding suggests

Table IV. Frequencies of the genotypic patterns of single-gland samples in gastric tumor, gastric intestinal metaplastic glands, and nonmetaplastic glands according to the genotype of pooled-gland samples.

Genotype of pooled-gland samples	Tumor (n-20)					Intestinal metaplastic gland (n-20)					Nonmetaplastic gland (n-10)				
	I	II	III	IV	V	I	II	III	IV	V	I	II	III	IV	V
Major	8	6	0	1	0	0	0	0	0	0	0	0	0	0	0
Minor	0	2	1	2	0	1	9	0	8	2	0	2	0	6	2

that genetic analysis of single intestinal metaplastic glands may be helpful in detecting such genetic alterations.

Marked clinical and biological heterogeneity has been noted among human gastric cancers (1-3). However, possible genetic causes of genetic heterogeneity have not been fully investigated. In this study, we used tumor single-gland samples to look for heterogeneous populations within the same tumor. Our findings that 90% of tumors demonstrated heterogeneous composition within the same tumor, show that gastric cancers are genetically highly complex. On average, there were 4.2 genetic alterations per tumor. The high number of genetic alterations per tumor indicates that genetic instability may cause intratumoral heterogeneity, as seen in other human tumors (1,3,27,28), and be an underlying mechanism of gastric carcinogenesis. In addition, our findings suggest that a specific subclone cannot be selected in most gastric cancers during tumor progression. This is an important finding toward understanding the effectiveness of chemotherapy or radiotherapy in gastric cancers, because the existence of heterogeneous populations indicates no single target cell can be defined.

The degree of accumulated LOH (allelic imbalance) has been shown to be of prognostic value in various cancer types including gastric cancer, and a high degree of tumor LOH has been shown to be associated with tumor aggressiveness and a worse prognosis (29). In light of these findings, low and high rates of tumor LOH suggest low and high tumor behavioral aggressiveness, respectively. In some of the present cases, although minor-altered genotype (low LOH) was found in the pooled-gland sample, major-altered genotype (high LOH) was detected in the corresponding tumor single-gland sample. Our findings also indicate that 2 of 5 tumors showing a minor-altered genotype in the pooled-gland sample were classified as type II (composed of major-altered genotype) in the tumor single-gland sample. This finding suggests that highly aggressive subclones may exist within a tumor showing a low frequency of LOH in a pooled-gland sample (2/5, 40%). It is surprising that 40% of pooled-gland samples showing the minor-altered genotype contained a major-altered genotype in the corresponding tumor single-gland samples. On the other hand, in the present study, most of the carcinomas that were examined contained a minor-altered genotype of single tumor glands within the same tumor. One recent study has shown that high-LOH tumors may have a higher rate of response to chemotherapy (29,30). However, in general, the majority of patients with gastrointestinal cancers are thought to obtain a poor response to chemotherapy without survival benefit (29,30). Although the genetic reason for the discrepancy remains unknown, an explanation may be that the minor-altered genotype gland is a supply source to the major-altered genotype gland. Therefore, a minor-altered genotype gland may co-exist with a major-altered genotype gland within the same tumor (3).

In the present study, genotypic pattern for a single-gland sample was classified into 5 groups. Although types I and II were the most frequent genotypic patterns (17/20, 85%), type IV, a tumor genotype showing predominantly minor-altered glands, was relatively rare (3/20, 15%). These findings suggest that single tumor glands with multiple genetic alterations may cause subclonal expansions in different areas within the same tumor, leading to occupation of the whole tumor mass in gastric cancers.

The general strategy of identification of individuals at high risk for progression to cancer offers promising possibilities for cancer prevention, and this approach largely depends on early detection. Therefore, it is important to evaluate GIM, which is generally thought to be a precancerous condition in gastric cancer (12,18). Furthermore, a previous study has shown that GIM is closely associated with *Helicobacter pylori* infection (31). However, little is known about the genetic events responsible for initiation and progression of gastric cancer (32,33). According to an investigation by Ochiai *et al*, although *p53* mutations known to play a key role in human neoplastic progression were identified in GIM, they were detected in only 10 of 756 (1.3%) histological sections (18). This finding indicates that it is difficult to identify such subtle genetic alterations in intestinal metaplastic glands. Genetic analysis of a single gland may enable us to identify subtle genetic alterations in GIM. Therefore, we used isolated single glands in the current study to address the issue of whether molecular alterations occur in GIM. In this study, although no genetic alterations were detected in pooled samples of intestinal metaplastic glands, alterations were frequently found in the corresponding single intestinal metaplastic gland samples. This suggests that intestinal metaplastic glands have a markedly heterogeneous composition. This study is the first to identify that expansive microsatellite alterations are seen in samples of intestinal metaplastic glands. These data indicate that irreversible genetic changes have already occurred in morphologically non-neoplastic gastric mucosa with intestinal metaplasia, and they support the hypothesis that GIM may be a precursor lesion of gastric cancer.

The present study has demonstrated that multiple genetic alterations are frequently found in nonmetaplastic glands. This is a surprising finding and the first study to identify genetic alterations in histologically normal gastric glands. This finding suggests that accumulation of genetic alterations occurs not only in metaplastic glands but also in nonmetaplastic glands, and that genetic alterations in gastric epithelial cells during chronic gastritis may contribute to an increased risk of gastric cancer (34).

In conclusion, single tumor glands can be useful for investigating genetic alterations in gastric cancers and gastric intestinal metaplasia. The present data indicate that most carcinomas and GIM are genetically heterogeneous. Recently, public policy strategies have been suggested for identification of patients at risk for *H. pylori*-related gastric malignancy (35,36). The thrust of this policy is that eradication of *H. pylori* infection earlier rather than later in life is anticipated to be more beneficial, because gastric intestinal metaplasia is expected to occur later in life. Our finding that multiple genetic alterations are found in single intestinal metaplastic glands may support this opinion.

Acknowledgements

We gratefully acknowledge the technical assistance of Miss E. Sugawara and Mr. T. Kasai. We also thank members of the Division of Pathology, Central Clinical Laboratory, Iwate Medical University, for their support.

References

1. Nowel PC: The clonal evolution of tumor cell populations. Science 194: 23-28, 1976.
2. Ishii M, Sugai T, Habano W and Nakamura S: Analysis of Ki-ras gene mutations within the same tumor using a single tumor crypt in colorectal carcinomas. J Gastroenterol 39: 544-549, 2004.
3. Sugai T, Habano W, Jiao Y-F, *et al*: Analysis of allelic imbalances at multiple cancer-related chromosomal loci and microsatellite instability within the same tumor using a single tumor gland from colorectal carcinomas. Int J Cancer 114: 337-345, 2005.
4. Fearon ER and Vogelstein B: A genetic model for colorectal tumorigenesis. Cell 61: 759-767, 1990.
5. Chung YJ, Kim KM, Choi JR, Choi SW and Rhyu MG: Relationship between intratumor histological heterogeneity and genetic abnormalities in gastric carcinoma with microsatellite instability. Int J Cancer 82: 782-788, 1999.
6. Iwamatsu H, Nishikura K, Watanabe H, *et al*: Heterogeneity of p53 mutational status in the superficial spreading type of early gastric carcinoma. Gastric Cancer 4: 20-26, 2001.
7. Sugai T, Uesugi N, Habano W, *et al*: DNA mapping of gastric cancers using flow cytometric analysis. Cytometry 42: 270-276, 2000.
8. Nakayama S, Nakayama K, Takebayashi Y, *et al*: Allelotypes as potential prognostic markers in ovarian carcinoma treated with cisplatin-based chemotherapy. Int J Mol Med 11: 621-625, 2003.
9. Barratt PL, Seymour MT, Stenning SP, *et al*: UKCCCR AXIS trial collaborators. Adjuvant X-ray and Fluorouracil Infusion Study. UKCCCR AXIS trial collaborators. DNA markers predicting benefit from adjuvant fluorouracil in patients with colon cancer: a molecular study. Lancet 360: 1381-1391, 2002.
10. Day DW, Jass JR, Price AB, Shepherd NA, Sloan JM, Talbot IC, Warren BF and Williams GT (eds): Morson and Dawson's Gastrointestinal Pathology. 4th edition, Blackwell Science, 114-115, 2003.
11. Mutoh H, Sakurai S, Satoh K, *et al*: Development of gastric carcinoma from intestinal metaplasia in Cdx2-transgenic mice. Cancer Res 64: 7740-7747, 2004.
12. Morgan C, Jenkins GJ, Ashton T, *et al*: Detection of p53 mutations in precancerous gastric tissue. Br J Cancer 89: 1314-1319, 2003.
13. Tatematsu M, Tsukamoto T and Mizoshita T: Role of *Helicobacter pylori* in gastric carcinogenesis: The origin of gastric cancers and heterotopic proliferative glands in Mongolian Gerbils. Helicobacter 10: 97-106, 20056.
14. Baracchini P, Fulcheri E and Lapertosa G: Patterns of intestinal metaplasia in gastric biopsies. A comparison of different histochemical classifications. Histochem J 23: 1-9, 1991.
15. Matsukura N, Suzuki K, Kawachi T, *et al*: Distribution of marker enzymes and mucin in intestinal metaplasia in human stomach and relation to complete and incomplete types of intestinal metaplasia to minute gastric carcinomas. J Natl Cancer Inst 65: 231-240, 1980.
16. Mirza ZK, Das KK, Slate J, *et al*: Gastric intestinal metaplasia as detected by a monoclonal antibody is highly associated with gastric adenocarcinoma. Gut 52: 807-812, 2003.
17. Blok P, Craanen ME, Offerhaus GJ and Tytgat GN: Gastric carcinoma: clinical, pathogenic, and molecular aspects. QJM 90: 735-749, 1997.
18. Ochiai A, Yamauchi Y and Hirohashi S: p53 mutations in the non-neoplastic mucosa of the human stomach showing intestinal metaplasia. Int J Cancer 69: 28-33, 1996.
19. Sugai T, Habano W, Nakamura S, *et al*: Genetic alterations in DNA diploid, aneuploid and multiploid colorectal carcinomas identified by the crypt isolation technique. Int J Cancer 88: 614-619, 2000.
20. Arai T and Kino I: Morphometrical and cell kinetic studies of normal human colorectal mucosa: Comparison between the proximal and the distal large intestine. Acta Pathol Jpn 39: 725-730, 1989.
21. Japanese Research Society for Gastric Cancer: The General Rules for the Gastric Cancer Study. 12th edition, Kanehara-Shuppan, Tokyo, pp64-89, 1993.
22. Nakamura S, Goto J, Kitayama M and Kino I: Application of the crypt-isolation technique to flow-cytometric analysis of DNA content in colorectal neoplasms. Gastroenterology 106: 100-107, 1994.
23. Sugai T, Habano W, Uesugi N, *et al*: Three independent genetic profiles based on mucin expression in early differentiated-type gastric cancers - a new concept of genetic carcinogenesis of early differentiated-type adenocarcinomas. Mod Pathol 17: 1223-1234, 2004.
24. Jiao Y-F, Sugai T, Habano W, Suzuki M, Takagane A and Nakamura S: Analysis of microsatellite alterations in gastric carcinoma by applying the crypt isolation technique. J Pathol 204: 200-207, 2004.
25. Habano W, Sugai T, Nakamura S and Yoshida T: A novel method for gene analysis of colorectal carcinomas using a crypt isolation technique. Lab Invest 74: 933-940, 1996.
26. Sugai T, Takahashi H, Habano W, *et al*: Analysis of genetic alterations, classified according to their DNA ploidy pattern, in the progression of colorectal adenomas and early colorectal carcinomas. J Pathol 200: 168-176, 2003.
27. Faquin WC, Fitzgerald JT, Boynton KA and Mutter GL: Intratumoral genetic heterogeneity and progression of endometrioid type endometrial adenocarcinomas. Gynecol Oncol 78: 152-157, 2000.
28. Matsumoto T, Fujii H, Arakawa A, *et al*: Loss of heterozygosity analysis shows monoclonal evolution with frequent genetic progression and divergence in esophageal carcinosarcoma. Hum Pathol 35: 322-327, 2004.
29. Grundei T, Mueller J, Scholz M, *et al*: Loss of heterozygosity and microsatellite instability as predictive markers for neoadjuvant treatment in gastric carcinoma. Clin Cancer Res 6: 4782-4788, 2000.
30. Ott K, Vogelsang H, Ott K, *et al*: Chromosomal instability rather than p53 mutation is associated with response to neoadjuvant cisplatin-based chemotherapy in gastric carcinoma. Clin Cancer Res 9: 2307-2315, 2003.
31. Hirayama F, Takagi S, Yokoyama Y, Yamamoto K, Iwao E and Haga K: Long-term effects of *Helicobacter pylori* eradication in Mongolian gerbils. J Gastroenterol 37: 779-784, 2002.
32. Boussioutas A, Li H, Liu J, *et al*: Distinctive patterns of gene expression in premalignant gastric mucosa and gastric cancer. Cancer Res 63: 2569-2577, 2003.
33. Sugai T, Habano W, Nakamura S, *et al*: Correlation of histological morphology and tumor stage with molecular genetic analysis using microdissection in gastric carcinomas. Diagn Mol Pathol 7: 235-240, 1998.
34. Yao Y, Tao H, Park DI, Sepulveda JL and Sepulveda AR: Demonstration and characterization of mutations induced by *Helicobacter pylori* organisms in gastric epithelial cells. Helicobacter 11: 272-286, 2006.
35. Hunt RH: Will eradication of *Helicobacter pylori* infection influence the risk of gastric cancer? Am J Med 117 (Suppl 5A): S86-S91, 2004.
36. Yoo EJ, Park SY, Cho NY, Kim N, Lee HS and Kang GH: *Helicobacter pylori*-infection-associated CpG island hypermethylation in the stomach and its possible association with polycomb repressive marks. Virchows Arch 452: 515-524, 2008.

Oncogene (2010) 29, 3723–3731

www.nature.com/onc

ONCOGENOMICS

Array-based genomic resequencing of human leukemia

Y Yamashita[1], J Yuan[2], I Suetake[3], H Suzuki[4], Y Ishikawa[5], YL Choi[1,6], T Ueno[1], M Soda[1], T Hamada[1], H Haruta[1], S Takada[1], Y Miyazaki[7], H Kiyoi[8], E Ito[9], T Naoe[5], M Tomonaga[7], M Toyota[10], S Tajima[3], A Iwama[2,11] and H Mano[1,6,11]

[1]Division of Functional Genomics, Jichi Medical University, Tochigi, Japan; [2]Department of Cellular and Molecular Medicine, Graduate School of Medicine, Chiba University, Chiba, Japan; [3]Laboratory of Epigenetics, Institute for Protein Research, Osaka University, Osaka, Japan; [4]First Department of Internal Medicine, Sapporo Medical University, Hokkaido, Japan; [5]Department of Hematology and Oncology, Nagoya University Graduate School of Medicine, Nagoya, Japan; [6]Department of Medical Genomics, Graduate School of Medicine, The University of Tokyo, Tokyo, Japan; [7]Department of Molecular Medicine and Hematology, Nagasaki University Graduate School of Biomedical Sciences, Nagasaki, Japan; [8]Department of Infectious Diseases, Nagoya University School of Medicine, Nagoya, Japan; [9]Department of Paediatrics, Hirosaki University Graduate School of Medicine, Aomori, Japan; [10]Department of Biochemistry, Sapporo Medical University, Hokkaido, Japan and [11]CREST, Japan Science and Technology Agency, Saitama, Japan

To identify oncogenes in leukemias, we performed large-scale resequencing of the leukemia genome using DNA sequence arrays that determine ~9 Mbp of sequence corresponding to the exons or exon–intron boundaries of 5648 protein-coding genes. Hybridization of genomic DNA from CD34-positive blasts of acute myeloid leukemia ($n = 19$) or myeloproliferative disorder ($n = 1$) with the arrays identified 9148 nonsynonymous nucleotide changes. Subsequent analysis showed that most of these changes were also present in the genomic DNA of the paired controls, with 11 somatic changes identified only in the leukemic blasts. One of these latter changes results in a Met-to-Ile substitution at amino-acid position 511 of Janus kinase 3 (JAK3), and the JAK3(M511I) protein exhibited transforming potential both *in vitro* and *in vivo*. Further screening for *JAK3* mutations showed novel and known transforming changes in a total of 9 out of 286 cases of leukemia. Our experiments also showed a somatic change responsible for an Arg-to-His substitution at amino-acid position 882 of DNA methyltransferase 3A, which resulted in a loss of DNA methylation activity of >50%. Our data have thus shown a unique profile of gene mutations in human leukemia.

Oncogene (2010) **29**, 3723–3731; doi:10.1038/onc.2010.117; published online 19 April 2010

Keywords: resequencing; AML; JAK3; DNMT3A

Introduction

Leukemias are clonal disorders of hematopoietic stem cells or immature progenitors. Several subtypes of leukemia are associated with disease-specific karyotype anomalies in the malignant blasts. Most cases of acute promyelocytic leukemia a subtype of acute myeloid leukemia (AML), for instance, are associated with a t(15;17) chromosomal rearrangement that results in the production of the PML-RARA fusion-type oncoprotein (Tallman and Altman, 2008). Similarly, another subtype of AML is associated with a t(8;21) rearrangement, resulting in the production of the oncogenic RUNX1-CBFA2T1 protein (Nimer and Moore, 2004).

The karyotype of leukemic blasts is an important determinant of the long-term prognosis of affected individuals. AML with t(15;17), t(8;21) or inv(16) rearrangements thus constitutes a subgroup of leukemias with a 'favorable' karyotype, with a 5-year survival rate of >60%, whereas AML with an 'adverse' karyotype (monosomy 7, monosomy 5 or complex anomalies) has a 5-year survival rate of only <15% (Grimwade *et al.*, 1998). The prognosis of AML with a normal karyotype (constituting ~50% of all AML cases) is substantially worse than that with a favorable karyotype, with a 5-year survival rate of 24% (Byrd *et al.*, 2002), indicating that blasts with a normal karyotype may contain transforming genes generated as a result of (1) sequence alterations, (2) epigenetic abnormalities or (3) small chromosomal rearrangements not detectable by the G-banding technique. Indeed, several genes, including *NPM1* and *KIT*, have been found to be mutated and activated in AML blasts with a normal karyotype (Schlenk *et al.*, 2008).

The identification of transforming genes in AML will require large-scale resequencing of the blast genome. Although a new generation of sequencing technologies is now available, whole-genome resequencing of many samples remains a demanding task (Bentley *et al.*, 2008; Wheeler *et al.*, 2008). Although DNA microarray-based sequencing is suitable for analysis of multiple samples, currently available platforms are limited in the number of nucleotides that each array is able to probe. To overcome such limitations, we have now applied the extra-large arrays ('wafers') manufactured by Perlegen Sciences (Mountain View, CA, USA) (originally developed for typing of

Correspondence: Dr H Mano, Division of Functional Genomics, Jichi Medical University, 3311-1 Yakushiji, Shimotsukeshi, Tochigi 329-0498, Japan.
E-mail: hmano@jichi.ac.jp
Received 6 May 2009; revised 1 January 2010; accepted 17 March 2010; published online 19 April 2010

single-nucleotide polymorphisms) (Patil *et al*., 2001) to resequencing of the human genome. Our two-step analysis of human leukemia specimens ($n=20$) has identified a novel transforming mutation in the gene for Janus kinase 3 (JAK3) and a hypomorphic mutation in that for DNA methyltransferase 3A (DNMT3A).

Results

Sequencing strategy

Oligonucleotide probes on the sequencing wafer for the first phase of our study were designed to detect nonsynonymous nucleotide changes in the coding exons of the genome. Intronic sequences (GT in the splicing donor sequence AG-GT and AG in the splicing acceptor sequence AG-G) adjacent to coding exons were also interrogated with the wafer to capture splicing anomalies. Genes examined by the wafer included those known to be mutated in cancer and reported in the catalog of somatic mutations in cancer (COSMIC, http://www.sanger.ac.uk/genetics/cgp/cosmic) as of September 2006 ($n=338$) and those related to the regulation of DNA repair ($n=419$), chromatin structure ($n=299$), redox regulation ($n=102$), epigenetic regulation ($n=44$), cell signaling ($n=2490$), protein kinases ($n=314$), gene transcription ($n=797$), cell cycle ($n=297$), apoptosis ($n=312$), DNA replication ($n=144$) or other functions ($n=92$) (Figure 1a). A total of 5648 genes were thus analyzed with the wafer.

To efficiently isolate oncogenes generated by point mutation using our sequencing array, we selected leukemic blasts with a karyotype characterized by few chromosome anomalies and by few copy number variations of chromosomes, as determined by comparative genomic hybridization with single-nucleotide polymorphism-typing arrays (Supplementary Figure S1). We isolated 15 cases of *de novo* AML, 4 cases of AML that developed from myelodysplastic syndrome, and 1 case of myeloproliferative disorder negative for the JAK2(V617F) and MPL(W515L) mutations (Kralovics *et al*., 2005; Pikman *et al*., 2006) (Supplementary Table S1).

From each of these 20 individuals enrolled in the study, we purified immature blasts positive for the surface expression of CD34 (leukemic fraction) as well as a paired control fraction of mature T cells positive for the surface expression of CD4. Although monocytes-macrophages may also express a low level of CD4 at the cell surface, our magnetic bead-based purification system preferentially enriched mature T cells with a high level of CD4 expression; contamination of the mature T-cell fraction with monocytes-macrophages was judged to be <9% by flow cytometry (Supplementary Figure S2).

Given the potential presence of substantial numbers of unreported single-nucleotide polymorphisms in the human genome, we adopted a two-step analysis to select somatic changes (Figure 1b). In phase I, genomic DNA was isolated from the $CD34^+$ fraction, subjected to mid-range PCR amplification and hybridized with the wafer to examine ~9 Mbp of nucleotide sequence. In phase II, we constructed a smaller wafer to investigate only the

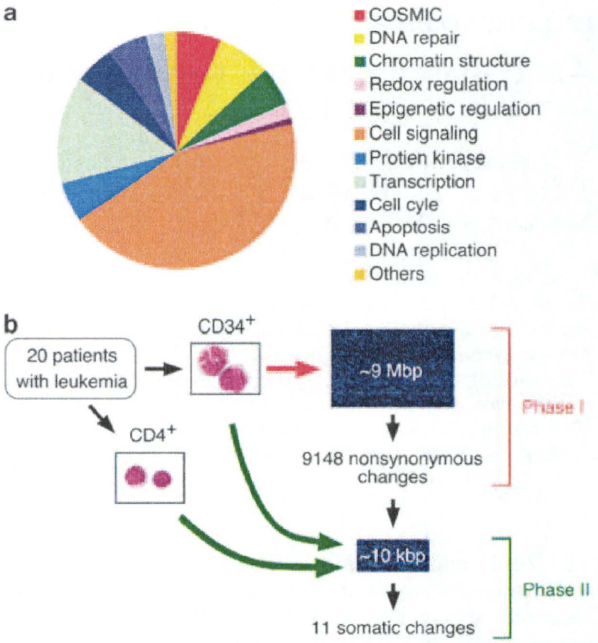

Figure 1 Resequencing of the leukemia genome with wafers. (**a**) Genes interrogated by the phase I wafer ($n=5648$) included those listed in the COSMIC database and those categorized on the basis of function of the encoded protein as indicated. (**b**) $CD34^+$ and $CD4^+$ cell fractions were purified from individuals with leukemia ($n=20$). Genomic DNA of the former fractions was assayed with the phase I wafer including ~9 Mbp of sequence, resulting in the isolation of 9148 nonsynonymous nucleotide changes in 3403 independent genes. The phase II wafer was then constructed to analyze these 9148 changes and was hybridized with genomic DNA from both $CD34^+$ and $CD4^+$ fractions separately. Only 11 mutations were found to be present in the former fraction but not in the latter.

nucleotides shown to be changed in phase I relative to the human reference sequence. Genomic DNA isolated from leukemic blasts and paired control fractions was then analyzed individually with the phase II wafer. We assumed that a nucleotide change was a germline polymorphism if it was observed in both leukemic and control fractions of the same individual, and that it was a somatic mutation if it was observed in the former fraction but not in the latter.

Identification of the JAK3(M511I) mutation

Screening of the leukemic blasts of the 20 individuals for point mutations in phase I yielded 9148 nonsynonymous changes among 3403 independent genes, a frequency similar to that observed in other large-scale resequencing studies performed with capillary sequencers (Sjoblom *et al*., 2006; Greenman *et al*., 2007). However, analysis of $CD4^+$ fractions showed that most of these sequence changes were also present in the paired control genome, leaving only 11 nonsynonymous somatic mutations in 11 genes (Supplementary Table S2). Such small number of somatic mutations is in a good agreement with the eight somatic mutations found in AML through whole-genome resequencing using the